

# We are IntechOpen, the world's leading publisher of Open Access books Built by scientists, for scientists

6,100

Open access books available

167,000

International authors and editors

185M

Downloads

Our authors are among the

154

Countries delivered to

TOP 1%

most cited scientists

12.2%

Contributors from top 500 universities



WEB OF SCIENCE™

Selection of our books indexed in the Book Citation Index  
in Web of Science™ Core Collection (BKCI)

Interested in publishing with us?  
Contact [book.department@intechopen.com](mailto:book.department@intechopen.com)

Numbers displayed above are based on latest data collected.  
For more information visit [www.intechopen.com](http://www.intechopen.com)



Chapter

# Investigations of Using an Intelligent ANFIS Modeling Approach for a Li-Ion Battery in MATLAB Implementation: Case Study

*Roxana-Elena Tudoroiu, Mohammed Zaheeruddin,  
Nicolae Tudoroiu and Sorin Mihai Radu*

## Abstract

This research paper will propose an incentive topic to investigate the accuracy of an adaptive neuro-fuzzy modeling approach of lithium-ion (Li-ion) batteries used in hybrid electric vehicles and electric vehicles. Based on this adaptive neuro-fuzzy inference system (ANFIS) modeling approach, we will show its effectiveness and suitability for modeling the nonlinear dynamics of any process or control system. This new ANFIS modeling approach improves the original nonlinear battery model and an alternative linear autoregressive exogenous input (ARX) polynomial model. The alternative ARX is generated using the least square errors estimation method and is preferred for its simplicity and faster implementation since it uses typical functions from the MATLAB system identification toolbox. The ARX and ANFIS models' effectiveness is proved by many simulations conducted on attractive MATLAB R2021b and Simulink environments. The simulation results reveal a high model accuracy in battery state of charge (SOC) and terminal voltage. An accurate battery model has a crucial impact on building a very precise adaptive extended Kalman filter (AEKF) SOC estimator. It is considered an appropriate case study of a third-order resistor-capacitor equivalent circuit model (3RC ECM) SAFT-type 6 Ah 11 V nominal voltage of Li-ion battery for simulation purposes.

**Keywords:** battery management system, Li-ion battery model, battery SOC, SOC UKF estimator, ANFIS model, ARX model, NMSS model, terminal voltage

## 1. Introduction

The most sustainable strategy to accomplish clean and efficient transport is to stimulate the automotive hybrid electric vehicles (HEVs)/electric vehicles (EVs) industry by developing the most advanced battery technologies. There is massive

competition in the markets for selling batteries with different chemistry, especially between the most common nickel-metal hydride (Ni-MH), nickel-cadmium (Ni-Cad) and lithium-ion (Li-ion) batteries. More recently, it seems that the most promising future and great potential of development for HEVs/EVs automotive industry worldwide have the Li-ion batteries due to their advantages compared with other strong competitors on the market. They surpass these competitors by features such as lightweight, high-energy-density, little memory effect, and relatively low self-discharge, as is mentioned in [1, 2]. Furthermore, after substantial improvements and research investments, the Li-ion batteries have become safer and less toxic. The battery state of charge (SOC) represents the available capacity of the battery cell that changes corresponding to the fluctuations in the input charging and discharging current profile during a cycle. It is worth mentioning that the SOC plays a crucial role in keeping the battery safe for various operating conditions and significantly extending battery life [3, 4]. Moreover, the SOC is an essential internal battery parameter of great significance constantly monitored by the battery management system (BMS) [1–6]. In real life, a specialized software package integrated onboard the vehicle estimates the value of the battery SOC due to the lack of an accurate measurement sensor integrated into BMS [1–7]. Let us see why the battery SOC has become a topic of great interest for researchers working in the field, very dedicated for developing the most suitable estimation techniques and strategies supported today by an impressive number of research papers published in the literature. The most used model-based Kalman filter (KF) can estimate the battery SOC with a high accuracy grade [3–7]. The BMS monitors the battery system through sensors and state estimation algorithms to detect any abnormalities during the battery system operation [8, 9]. The performance of the battery SOC estimators' model is highly dependent on the battery model accuracy. If the battery model is accurate, then the different SOC estimation versions will estimate the battery SOC with the same accuracy. Consequently, the battery model is essential for implementing the most suitable SOC estimators. It is always desirable to get a battery model as accurate as the actual battery to reduce the mismatch between the model and the existing battery. Moreover, the battery SOC is “a critical factor in guaranteeing that a battery system operates safely and reliably,” as is mentioned in [10]. Also, “many uncertainties and noises, such as current, sensor measurement accuracy and bias, temperature effects, calibration errors or even sensor failure, etc., pose a challenge to the accurate estimation of SOC in real applications” [10].

Additionally, over time, the effects of battery aging will be more noticeable in degrading its performance, and the mismatch between the battery model and the actual battery will also increase. In the “real-life” applications subjected to the plant/process identification, fixing the possible mismatches between the plant/process and their corresponding models with repeated effective re-identification procedures is almost inapplicable and time-consuming, as is revealed in [10–12]. Therefore, mismatch detection is essential for different plants/processes modeling and identification strategies to isolate defective submodules to avoid complete re-identification, as mentioned in [11].

### **1.1 State-of-the-art Li-ion battery models and SOC estimators**

A suitable identification plant/process strategy is developed in [10–12] that is a polynomial discrete state-space representation of the plant/process models based on a

plant/process input-output measurement data set collected in an open loop. The plant/process input-output measurement data set is used to develop and implement two attractive statistical models.

The first model is a linear discrete state-space autoregressive exogenous input (ARX) polynomial representation, beneficial to model a 60 Ah LiFePO<sub>4</sub> battery module [10]. Based on this model, an extended Kalman filter (EKF) battery SOC estimator is developed for BMSs. The second model is an auto-regressive moving average with exogenous input (ARMAX) model developed in [12]. The adaptability of ARX battery models developed in [10] for designing a robust and accurate EKF SOC estimator is rigorously assessed in the same reference [10]. Some simulation results indicate that the proposed EKF SOC battery module estimator based on the ARX model shows a “great performance” in terms of robustness and SOC accuracy [10]. Additionally, the proposed EKF battery estimator “increases the model output voltage accuracy, thereby having the potential to be used in real applications, such as EVs and HEVs” [10]. Two MIMO ARMAX models are developed in [12] for modeling and identification of heating, ventilation, and air-conditioning (HVAC) multi-input multi-output (MIMO) centrifugal chiller plant. This model is built and implemented in a MATLAB simulation environment to develop two accurate MIMO proportional integral-plus (PIP) control strategies in a closed loop for temperature control and refrigerant liquid control level. For comparison purposes in [11], ARX and ARMAX polynomial discrete-time plant representations are built as decorrelation models for detecting model-plant mismatch for a column distillation integrated into a model predictive control (MPC) strategy. Detailed simulations in [11] show that the ARMAX models provide:

- Higher accuracy
- Less computational complexity
- Less processing power is required with less model order than ARX.

Moreover, in [12], ARMAX models are developed for an MIMO HVAC centrifugal chiller open-loop control system using the identification techniques presented in MATLAB Identification Toolbox [13]. Also, for the same HVAC plant, an MIMO ARMAX open-loop polynomial model helps implement an interesting closed-loop proportional integral-plus (PIP) control strategy of chiller plant temperature and liquid-level refrigerant. Both ARX and ARMAX models are helpful in [12] for implementing an extended MIMO PIP control strategy as a new modeling approach in a non-minimal discrete-time state-space system representation (NMSS). The MATLAB simulation results show a superior accuracy of the MIMO NMSS centrifugal chiller model compared with the ARMAX models. Therefore, the MIMO PIP closed-loop control strategy based on the MIMO NMSS models performs better than those built on the MIMO ARMAX models of the MIMO chiller plant, as is proved in [12, 13].

Taking advantage of the considerable advances in modeling, identification, and control systems developed in the field of literature, thanks to the latest achievements in artificial intelligence, statistics and machine learning, deep learning, signal process analysis, our research objectives diversify with new approaches. The most recent results in modeling and identification for various industrial applications reported in the literature field motivate us to investigate attractive new modeling approaches.

Then remains to adapt these approaches to our research topic of developing new Li-ion battery models. Furthermore, the proposed Li-ion battery SOC estimator for a Rint SAFT model of 6 Ah and 11 V nominal voltage in the selected case study is expected to perform much better in terms of accuracy and robustness of the battery SOC estimates for different operating conditions [7]. For simulation and comparison results purposes, as a case study of Li-ion battery, a third-order resistor-capacitor (RC) equivalent circuit model (ECM) (in abbreviated notation 3RC ECM) is considered. It combines three parallel polarization circuits R-C connected in series with the battery's internal resistance (Rint) and voltage source, i.e., as a similar 3RC ECM battery model developed in [7]. The model selection is suggested due to its simplicity and ability to describe the static and dynamic behavior of the Li-ion battery accurately.

Since the proposed Li-ion battery's open-circuit voltage (OCV) has highly nonlinear dependence on the battery SOC, as an alternative block model developed in [7], it is an adaptive neuro-fuzzy inference system (ANFIS) model. It is a hybrid neuro-fuzzy technique that brings the learning capabilities of neural networks to fuzzy inference systems. The learning algorithm tunes the membership functions of a Sugeno-type fuzzy inference system using the training input/output data [14]. More precisely, the learning algorithm teaches the ANFIS to map the input (current driving cycle profile) to the Li-ion battery SOC and terminal voltage through training. At the end of the training, the trained ANFIS network would have learned the input-output map and be ready to be deployed into the Kalman filter SOC estimator solution. The architecture, design, and implementation of the proposed ANFIS battery model are developed in an attractive MATLAB R2021b simulation environment [14–16]. This new battery model adjusts the design techniques and guidelines inspired from [14–33] to the selected model adopted in the case study from [7]. The accuracy of the ANFIS battery model has a significant impact on the SOC Li-ion battery Kalman Filter estimator accuracy performance built on this model. Its effectiveness is proved through extensive simulations and comparisons conducted on the same MATLAB platform. In this research, our motivation for using adaptive neuro-fuzzy training of Sugano-type fuzzy inference system (ANFIS) modeling comes from the preliminary results obtained for similar investigations on the impact of nonlinearities and uncertainties actuators [18]. The ANFIS modeling is well documented in the most recent MATLAB release versions that use the fuzzy logic toolbox and fuzzy inference tuning procedure [14–16]. Handy tutorials of using ANFIS modeling architectures are presented in [14–17]. For MATLAB implementation and simulation intent, as well as “proof concept” in this research, the accuracy of the Li-ion battery ANFIS model is tested for a battery urban dynamometer driving schedule (UDDS) input current profile.

In the proposed case study, for both ARX and ANFIS models an adaptive EKF (AEKF) SOC estimator is adopted attached to Li-ion battery used for creating fault detection and isolation (FDI) control strategies in [12], preferred for its simplicity, SOC accuracy, real-time implementation capability, and robustness. Its robustness is tested for four different scenarios, such as to changes in SOC initial values (guess values), ranging 70–40%, 20, 90, and 100%, to federal test procedure for 75 F (FTP-75) degree Fahrenheit driving cycle profile test, changes in measurement-level noise (from 0.001 to 0.01), to changes in the battery capacity value from 6 Ah to 4.8 Ah due to aging effects, and changes in internal resistance due to temperature effects, and also for simultaneous changes [7, 29]. Based on a rigorous performance

analysis of SOC residual error compared with the similar results reported in the literature with a typically 2% error, in some situations, the AEKF estimator SOC residual error reached values smaller than 1%, such as shown in [29]. Since of the lack of data in the literature field for similar situations developed in our research for Li-ion battery, it is not easy to make a state-of-the-art analysis of the results reported in the literature related to Li-ion battery SAFT 6 Ah and 11 V nominal voltage AEKF SOC estimators based on ANFIS models analysis. The overall ANFIS battery model consists of two ANFIS models, the first one attached to the battery Rint-3RC active part and the second to OCV(SOC) nonlinear block. The SOC and terminal voltages accuracy of the overall battery ANFIS model and AEKF SOC estimators, as well as their robustness to changes in the initial values of the battery SOC from 70 to 40%, are proved in this research paper based on extensive simulations conducted on MATLAB R2021b platform.

### **1.2 Statistical criteria for evaluating the performance of Li-ion battery – SOC and terminal voltage**

Based on MATLAB simulation results useful information on SOC and battery terminal voltage accuracy can be extracted based on SOC and terminal voltage residuals and based on four statistic criteria values shown in eight tables, defined in [29, 30], and grouped as:

- Root mean squared error (RMSE)
- Mean squared error (MSE)
- Mean absolute error (MAE)
- Mean average percentage error (MAPE)

For each Li-ion battery model developed in this research, the SOC and terminal voltage performance are evaluated by simulations conducted on MATLAB Simulink platform. The information extracted from these simulations is beneficial for a rigorous comparison of performance, so that the reader has a better perspective on the modeling, design, and implementation of the battery. From a variety of battery models, the reader has the ability to decide which model and estimator are best for a particular application.

### **1.3 Manuscript structure, objectives, and performed results**

The paper is organized as follows: Section 2 gives a brief description of Rint Li-ion SAFT 6 Ah 11 V nominal voltage and battery selection for the case study, model option, and its validation using the National Renewable Energy Laboratory (NREL) ADVANCED SIMULATOR (ADVISOR) 2003 for HEVs and EVs design. An equivalent electric circuit model (ECM) for the Li-ion battery SAFT Rint model is preferred due to its simplicity and ability to capture all the battery dynamics such that its SOC and the predicted terminal cell voltage are of high accuracy. The dynamics battery part ARX and ANFIS models, the ANFIS battery OCV(SOC) model, their order

selection, parameters identification and model implementation, ANFIS models' generation and performance, and the MATLAB simulation results are shown and discussed in Sections 2 and 3, respectively. For the ARX model and hybrid combinations of the ARX model and ANFIS model of OCV(SOC) nonlinear block, an overall ANFIS battery model consisting of ANFIS dynamic battery part model and ANFIS OCV(SOC) nonlinear battery block models are considered. A rigorous analysis of AEKF SOC estimator adaptability for all these models is evaluated based on simulation results conducted on MATLAB R2021b and Simulink environments that provide valuable information on SOC and battery terminal voltage accuracy and robustness performance. Also, a comparison of the evaluation of the results is made based on the SOC and battery voltage residuals and statistics criteria values summarized in almost eight tables in the last subsection 2.1.3 of Section 2 and all Section 3. Section 4 is dedicated to Conclusions supporting all the previous MATLAB results. In summary, in this research paper an impressive number of investigations are done on the accuracy and adaptability of six alternative Li-ion batteries models to the original NREL Li-ion Rint SAFT-type 6 Ah 11 V rated voltage battery model. The main reason of this selection is that the Li-ion batteries are very common in a wide variety of HEVs/EVs applications in the automotive industry, Also, it is a beneficial option to be used as a baseline model of Li-ion battery for performance comparison and validation of alternative models, among them the linear, simple, and accurate 3RC ECM Li-ion battery model developed in this research work. This alternative model is designed by using one of the most used designing tools very spread in the automotive industry, created by NREL, known as ADVANCED SIMULATOR (ADVISOR) with the final launch in 2003 for HEVs/EVs design. The Li-ion battery model 3RC ECM model is selected for simulation purpose and "proof" concept for developing new alternative battery models. Five alternative models that derivate from 3RC ECM Li-ion battery model are developed in this research work: (a) ARX-ECM that models the dynamic part of the battery represented by the Rint-3RC circuit using an equivalent ARX model; (b) ANFIS-ECM replacing the Rint-3RC circuit with an ANFIS model; (c) ARX-ANFIS hybrid structure that is a combination of ARX model for Rint-3RC dynamic part and an ANFIS model of the nonlinear static block OCV (SOC); (d) Rint-3RC -ANFIS model that keeps the dynamic part of the battery combined with the ANFIS model of OCV(SOC) static block; (e) full ANFIS model structure derived from ARX-ANFIS, which replaces the ARX model with an ANFIS model. The MATLAB simulation results for each model provide a large database stored in 10 useful tables for a rigorous analysis of the performance of the Li-ion battery in terms of SOC accuracy and terminal voltage, as well as the robustness of the AEKF algorithm for estimating the SOC of the selected battery.

## **2. Li-ion battery selection, modeling, MATLAB implementation, and ADVISOR simulator experimental test setup validation**

### **2.1 Li-ion battery model selection, description, and validation: case study**

In this section, we focus our attention on the Li-ion battery selection for the case study, its description, and developing the most suitable battery model of high accuracy. The selected model is validated through an impressive number of simulations conducted on the MATLAB R2021b platform. Then will compare the MATLAB simulations result to an experimental test performed in a similar

MATLAB environment integrated with a specialized simulator ADVISOR for batteries design of different chemistry, which is very spread in the automotive industry. National Renewable Energy Laboratory (NREL) developed this simulator in 1983 and improved its performance until the last release in 2003-00-r0116. A 6 Ah nominal capacity and 11 V nominal voltage SAFT Li-ion battery integrated into the hybrid electric vehicle (HEV) BMS structure, namely a Japanese Toyota Prius, one of the most spread commercial hybrid electric cars on the automotive industry market. It is equipped with an MC-AC75 motor of 75 kW and a powertrain control version, TX-5SPD manual transmission with five speeds and frontal wheel drive, as shown in **Figure 1**. In this figure on the right side, the reader can see the type of vehicle in the database of the ADVISOR simulator considered one of its primary inputs; also, at the bottom side is shown the open-circuit voltage (OCV) graph of the proposed SAFT Li-ion battery as the most suitable for the HEV car selected in the case study.

**Figure 2** shows the Simulink diagram of the Toyota Prius HEV car configuration. In **Figure 3**, you can see the graphical user interface that selects the urban dynamometer driving schedule (UDDS) of cycle speed profile for a driving test, the initial temperature, state of charge (SOC), and the ambient conditions.

In **Figure 4**, the MATLAB simulations results are displayed. Among these results two of the variables of interest can be emphasized, such as the UDDS driving cycle input current profile (ess\_current) and the battery SOC evolution (ess\_soc\_hist).

The UDDS driving cycle of the current profile shown in **Figure 5** is the equivalent of the UDDS driving cycle speed profile shown in the graph in **Figure 3**. It represents

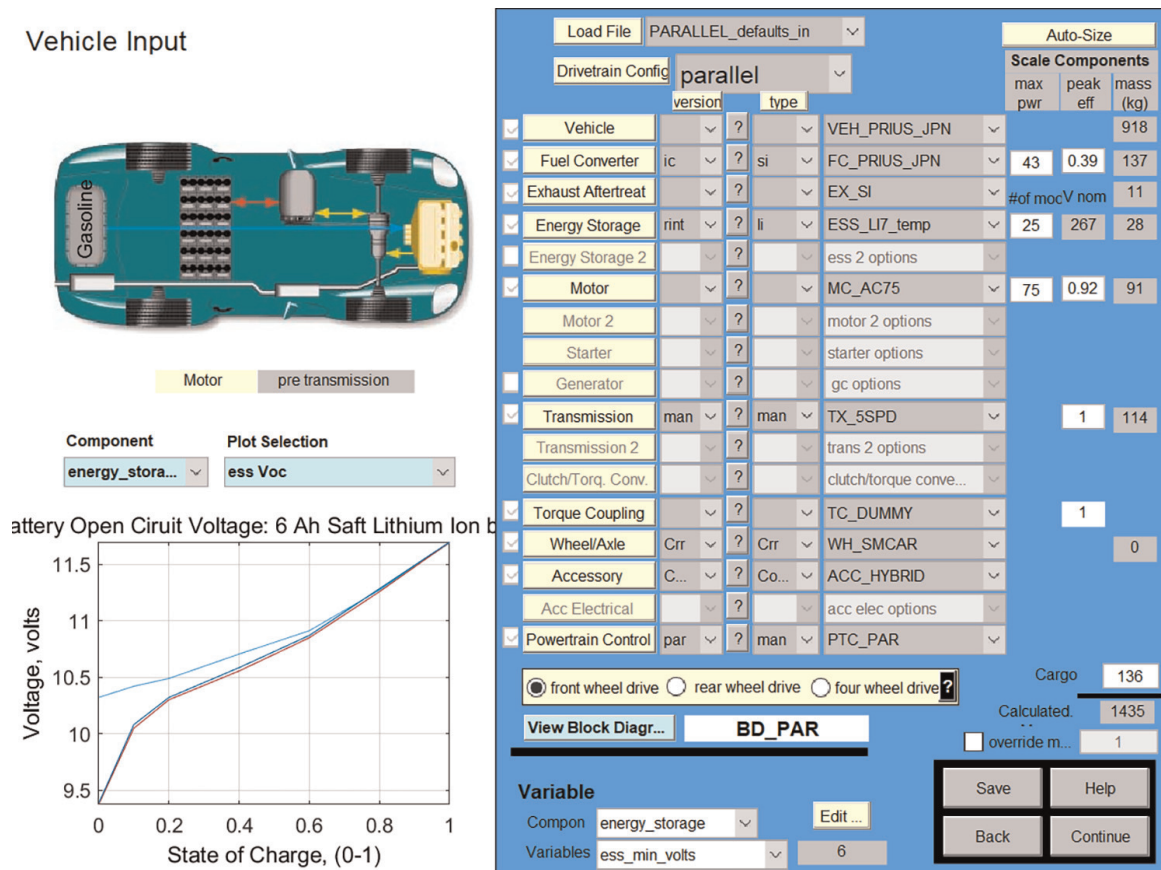


**Figure 1.**  
 The ADVISOR 3.2 simulator -input interface set up.



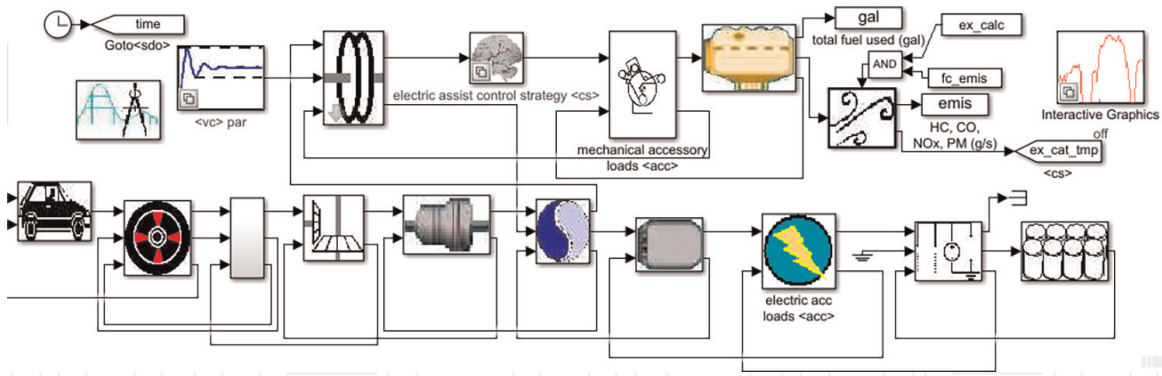


Figure 2. Block diagram of HEV powertrain configuration.

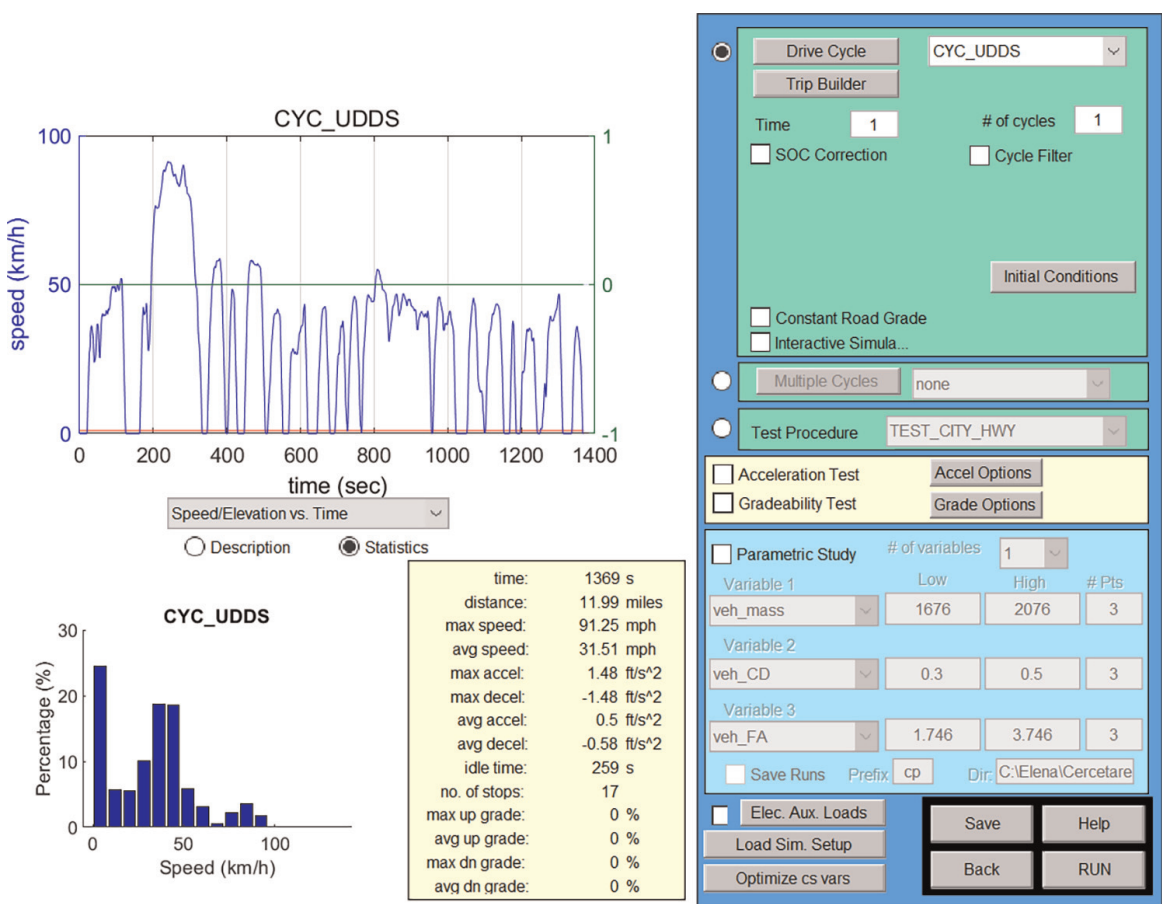


Figure 3. Graphical user interface with the ADVISOR simulator parameters.

the evolution of the input battery current during a repeated sequence of charging and discharging the battery for different periods.

More precisely, the ADVISOR 3.2 Simulator provides an extensive Database of different types of HEV cars, driving cycles speed tests, and input currents profiles for battery charging and discharging cycles.

### 2.1.1 Li-ion battery electrical equivalent circuit model

For simulation purposes and “proof concept,” a starting point for developing new Li-ion battery alternative models might be a linear electrical circuit consisting of one

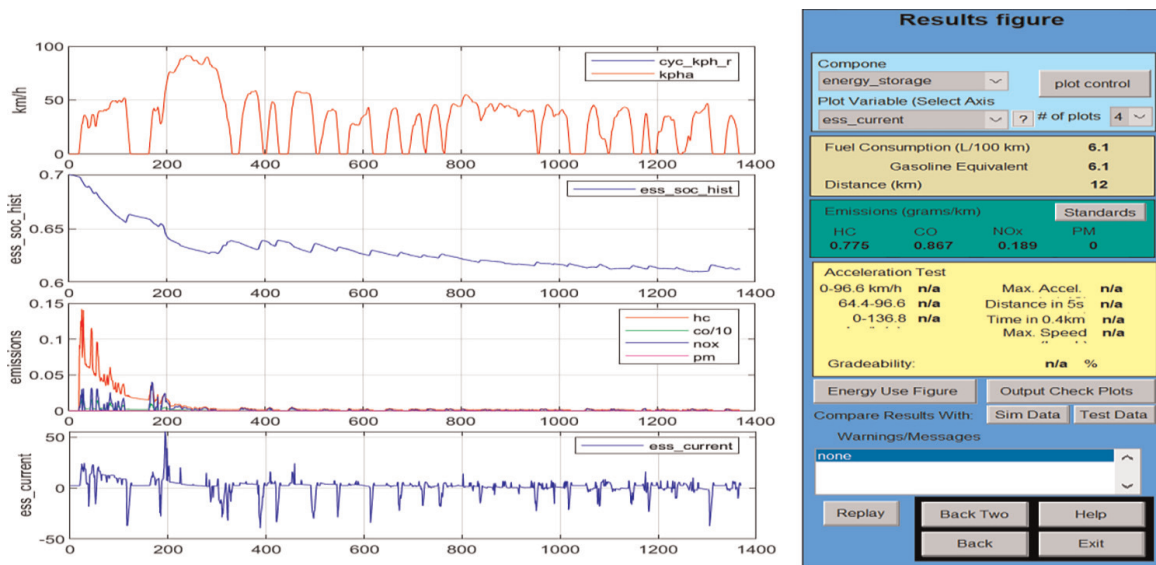


**Figure 4.**  
 MATLAB input-output simulation results.

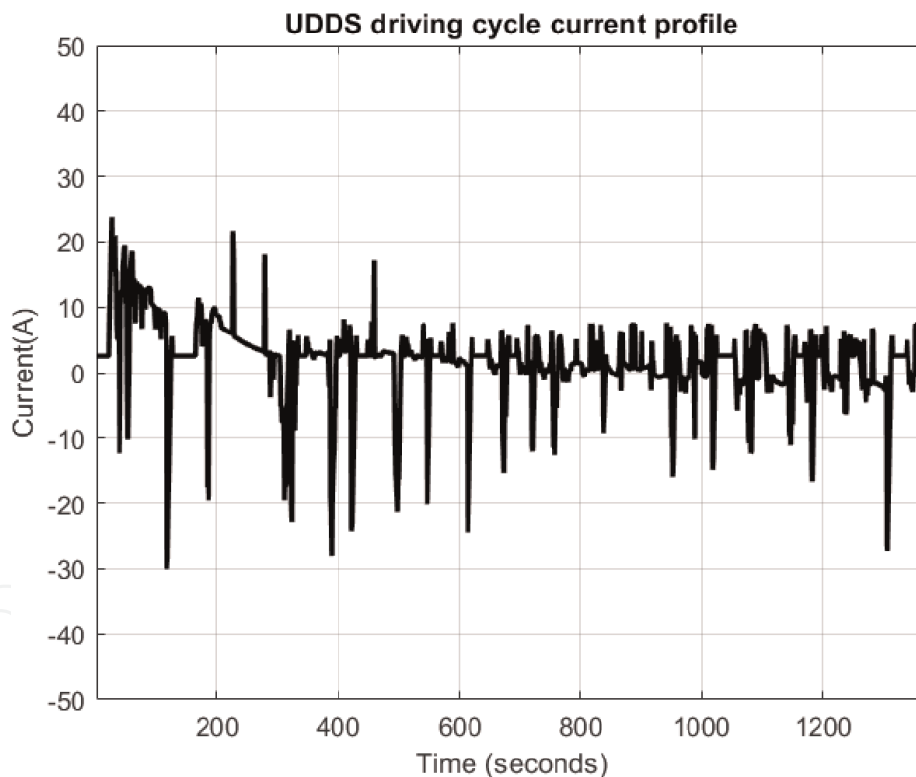


**Figure 5.**  
 The input UDDS driving cycle current profile (battery charging and discharging periods).

of the combinations of an open-circuit voltage (OCV) controlled source, known in the literature as Thevenin voltage source, connected in series with the internal resistance ( $R_{int}$ ) of the battery, followed by one, two, or three parallel resistive and capacitive polarization cells (RC). These combinations lead to a simple electrical equivalent circuit models (ECMs) very spread in the literature field as is shown in **Figure 6** [7]. Until now, the ECMs proved that they are of the high simplicity and are the most suitable models to capture the battery's dynamic electrochemical behavior and increase the model's accuracy. Since in **Figure 6**, the ECM has three parallel RC bias

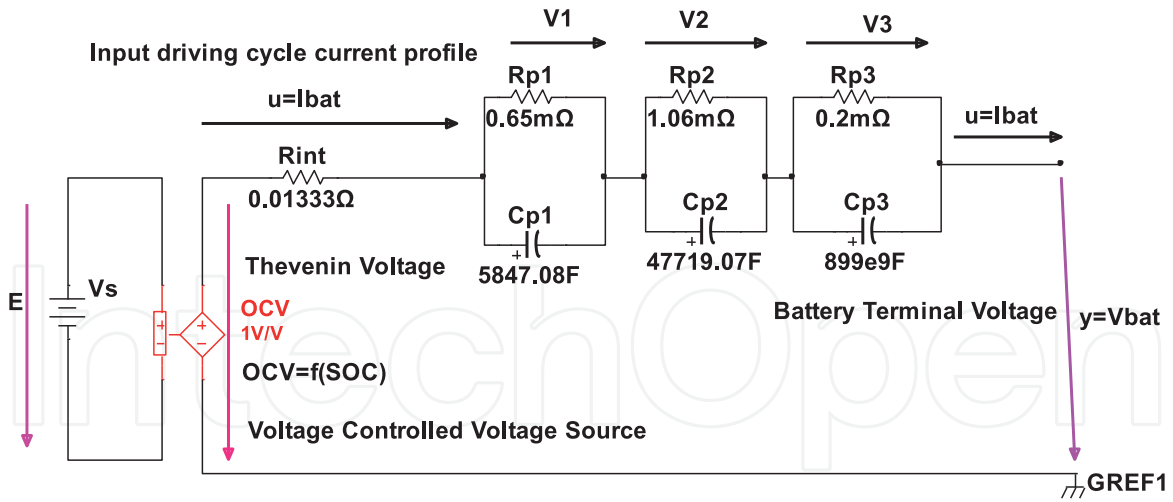


**Figure 6.** Electrical schematic of third-order 3RC ECM battery selection (see [7]).

polarization cells, it is known in the literature field as a three-order RC (3RC) ECM Li-ion battery model. The ECM schematic is built using the Multisim 14.1 software package provided by the well-known National Instruments (NI) company. The first R1pC1p polarization parallel cell captures the fast transient of the battery compared with the last two RC cells that capture only the slow steady state with a great impact in the increase of the battery model accuracy [7]. Since most HEV/EV technologies are very dependent on batteries nowadays, it is crucial for developing and implementing accurate Li-ion battery models. These models must suit better the BMS requirements to be easily deployed on-board power simulators and electronic on-board power systems. Moreover, the 3RC ECM accuracy performance is a baseline for all other alternative battery models developed in this research paper for comparison purposes. For MATLAB simulation’s goal, a similar setup for the 3RC ECM Li-ion battery model parameters used in [7], shown in **Table 1** or directly on the electrical schematics from **Figure 6**, is considered to prove the effectiveness and the robustness of an adaptive extended Kalman filter SOC estimation strategy, similar to those used in [9] for a generic Li-ion cobalt battery and adapted to the 3RC ECM model, presented in Appendix A. This setup is achieved from a generic ECM by changing only the values of the model parameters in state-space equations.

### 2.1.2 Li-ion battery 3RC ECM validation

The Li-ion battery 3RC ECM model parameters and the OCV nonlinear model coefficients are given in **Tables 1** and **2**. The OCV shown in **Figure 7** is a nonlinear function of SOC that combines three additional well-known models, namely Shepherd, Unnewehr universal and Nernst (SUN-OCV) models, defined in [3, 5, 7, 9] with the coefficients set at same values as in [3, 7, 9].

According to the values of the parameters and coefficients set in the **Table 1** the Li-ion battery model dynamics is described by the following discrete-time Eqs. [7]:

$$x_1(k + 1) = a_{11}x_1(k) + b_1u(k) = V_1(k) \quad (1)$$

$$x_2(k + 1) = a_{22}x_2(k) + b_2u(k) = V_2(k) \quad (2)$$

$$x_3(k + 1) = a_{33}x_3(k) + b_3u(k) = V_3(k) \quad (3)$$

Item	Parameters/Coefficients	Symbol	Value	Unit Measure
1	Li-ion battery ECM parameters			
1.1	Internal ohmic resistance	Rint+	13.333	mΩ (milliohm)
1.2	First cell polarization resistance	Rp1	0.65	mΩ
1.3	Second cell polarization resistance	Rp2	1.06	mΩ
1.4	Third cell polarization resistance	Rp3	0.2	mΩ
1.5	First cell polarization capacitance	Cp1	5847.08	F (Farad)
1.6	Second cell polarization capacitance	Cp2	47719.07	F
1.7	Third cell polarization capacitance	Cp3	8.99e9	F
2	Li-ion battery OCV coefficients			
2.1	k0			11.38
2.2	k1			3.86e-5
2.3	k2			0.24
2.4	k3			0.22
2.5	k4			0.04

**Table 1.**  
 The 3RC ECM parameters and OCV coefficients [3, 7, 9].

Criteria indices	Acronyms		Values
	ARX-ECM	ANFIS combined model	
IC1	RMSE	8%	2.2%
IC2	MSE	0.64%	0.051%
IC3	MAE	4.17%	1.1%
IC4	MAPE	8.12%	1.73%

**Table 2.**  
 Performance of the Li-ion AEKF SOC ARX model compared with AEKF SOC estimator ANFIS model for UDDS driving cycle test [7].

$$x_4(k+1) = x_4(k) + \frac{\eta T_s u(k)}{C_{nom}}, x_4(k) = SOC(k) = SOC(kT_s) \quad (4)$$

$$OCV(k) = k_0 - k_2 x_4(k) - \frac{k_1}{x_4(k)} + k \ln(x_4(k)) + k \ln(1 - x_4(k)) \quad (5)$$

$$y(k) = OCV(k) - R_{in} u(k) = V_{bat}(k), u(k) = I_{bat}(k) \quad (6)$$

where  $T_s = 1$  [s] is the sampling time, and the values of the equations' coefficients (1)–(6) are given by  $a_{11} = 1 - \frac{T_s}{T_1}$ ,  $a_{22} = 1 - \frac{T_s}{T_2}$ ,  $a_{33} = 1 - \frac{T_s}{T_3}$ ,  $a_{44} = 1$ ,  $b_1 = \frac{T_s}{C_{p1}}$ ,  $b_2 = \frac{T_s}{C_{p2}}$ ,  $b_3 = \frac{T_s}{C_{p3}}$ , and  $b_4 = -\frac{\eta T_s}{3600 Q_{nom}}$ . In the expression of the coefficient  $b_4$ ,  $\eta$  is the Coulombic efficiency, and  $Q_{nom}$  represents the nominal capacity of the battery, set to the following values:  $\eta = 0.85$ , and  $Q_{nom} = 6Ah$ . Also, the time constants of the polarization cells  $T_1, T_2$ , and  $T_3$  are given by:  $T_1 = R_{p1}C_{p1}$ ,  $T_2 = R_{p2}C_{p2}$ , and  $T_3 = R_{p3}C_{p3}$ .

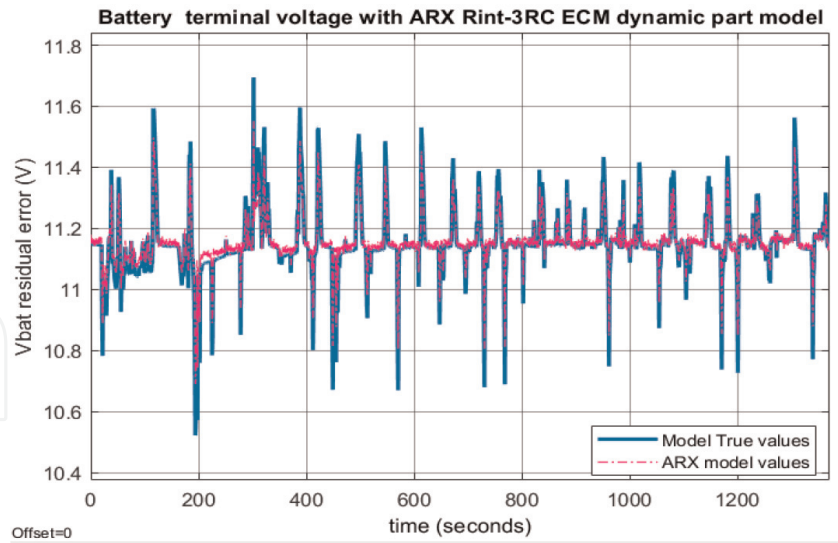


**Figure 7.** Battery terminal Rint-3RC ECM voltage versus ARX – ECM for the dynamic part of the battery.

A Simulink model based on these previous equations is shown in **Figure 8a**, compact in compact form, and in **Figure 8b**, for a detailed form.

The MATLAB simulation results are shown in **Figure 9**. In **Figure 9a** and **b** are depicted the SOC of the battery 3RC model versus SOC estimated by the ADVISOR simulator. In **Figure 9c** and **d** are presented the OCV =  $f(\text{SOC})$  curve and the battery SOC for a complete UDDS discharge cycle respectively. In **Figure 9e** is shown only the terminal voltage for a single UDDS cycle. The SOC residual represented in **Figure 9b** reveals a good SOC accuracy performance of the 3RC EMC battery model with respect to the estimated battery SOC on the ADVISOR simulator integrated with the MATLAB platform. This excellent result is a realistic argument that validates certainly the proposed 3RC ECM Li-ion battery attached to the generic Rint model of SAFT-type battery.

### 2.1.3 Li-ion battery 3RC ECM SOC estimation using an adaptive extended Kalman filter (AEKF)

The main goal of this section is to estimate the battery SOC and analyze the AEKF SOC estimator accuracy compared with the actual value of the battery model validated in the previous section. It is essential to prove that an accurate battery model in terms of SOC and terminal voltage is vital for building the most accurate SOC estimator. To accomplish this goal, an adaptive extended Kalman filter (AEKF) SOC estimator is adopted in this research, encouraged by the preliminary results obtained in [9, 29] by using the same AEKF estimator for a similar application. The SOC estimator implementation is performed on the MATLAB R2018b platform, and the simulation results are depicted in **Figure 10**. Also, in **Figure 10a** is shown the SOC AEKF estimator accuracy and its robustness to changes in the SOC initial value from  $\text{SOC}_{\text{ini}} = 0.7$  to  $\text{SOC}_{\text{ini}} = 0.4$ , compared with the 3RC ECM model values. In **Figure 10b**, the battery model terminal voltage is compared with the AEKF estimate of the terminal voltage. Both **Figure 10a** and **b** reveal that the SOC AEKF estimator performs well with high SOC accuracy, evaluated also based on their errors shown in **Figure 10c** and **d**.

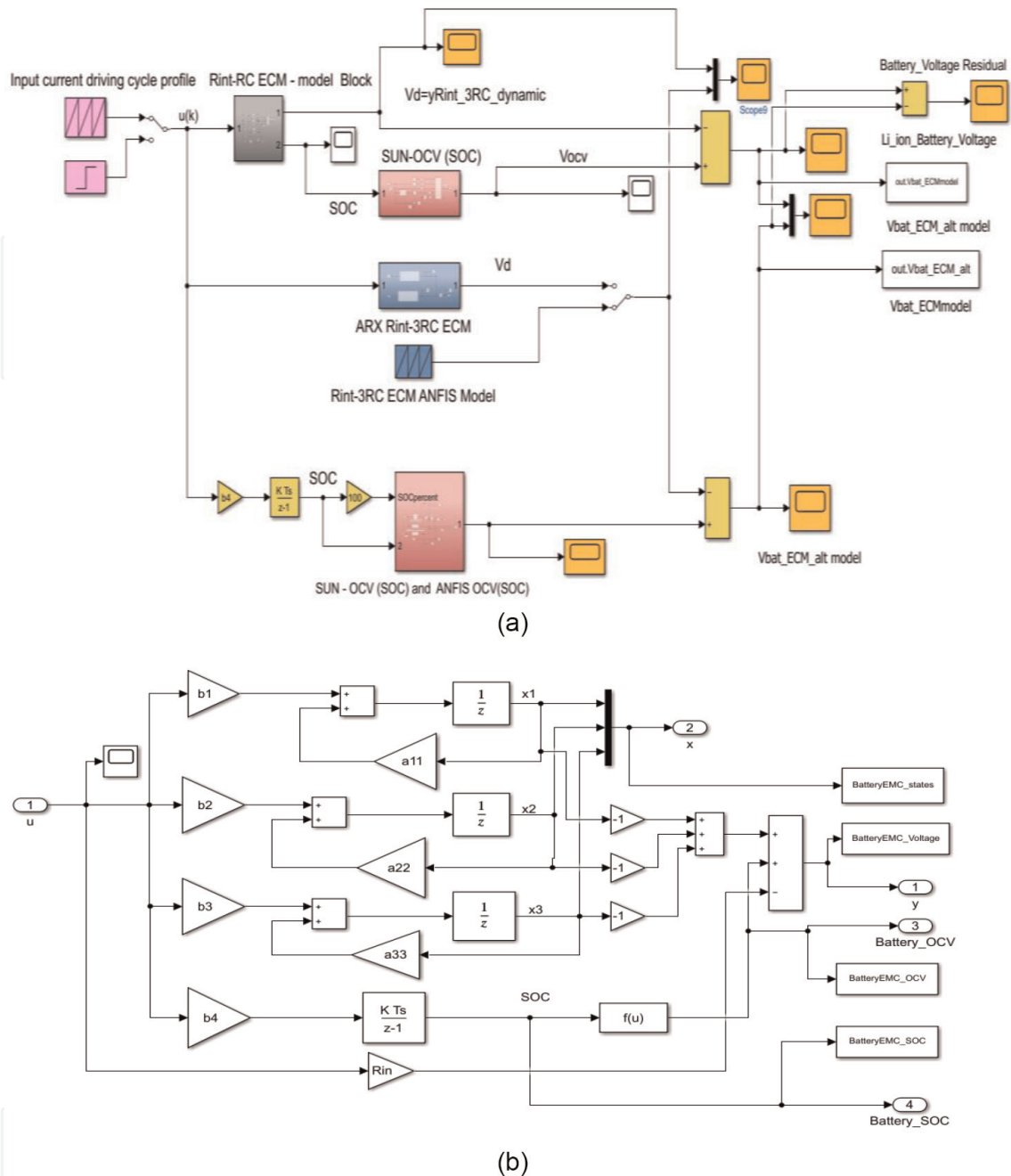


**Figure 8.** (a) The Simulink model of the 3RC ECM Li-ion battery in compact form; (b) the detailed Simulink model of the 3RC ECM Li-ion battery.

#### 2.1.4 The ARX model of the Rint-3RC ECM circuit dynamics (ARX-ECM)

An alternative to the battery model is a linear polynomial model in discrete-time state-space representation, namely an autoregressive with exogenous terms (ARX) model, which captures the dynamics impact on the series circuit Rint (internal battery resistance) and all three RC polarization cells. The linear discrete-time polynomial model ARX is one of the simplest models that incorporate the stimulus input signal to capture some stochastic dynamics as part of the 3RC ECM dynamics. Since the  $OCV = f(SOC)$  curve is of high nonlinearity, an ANFIS model is also assessed. A hybrid battery model structure ARX Rint-3RC ECM – ANFIS OCV(SOC) model will be developed as a challenge in this valuable research for the reader to have a good

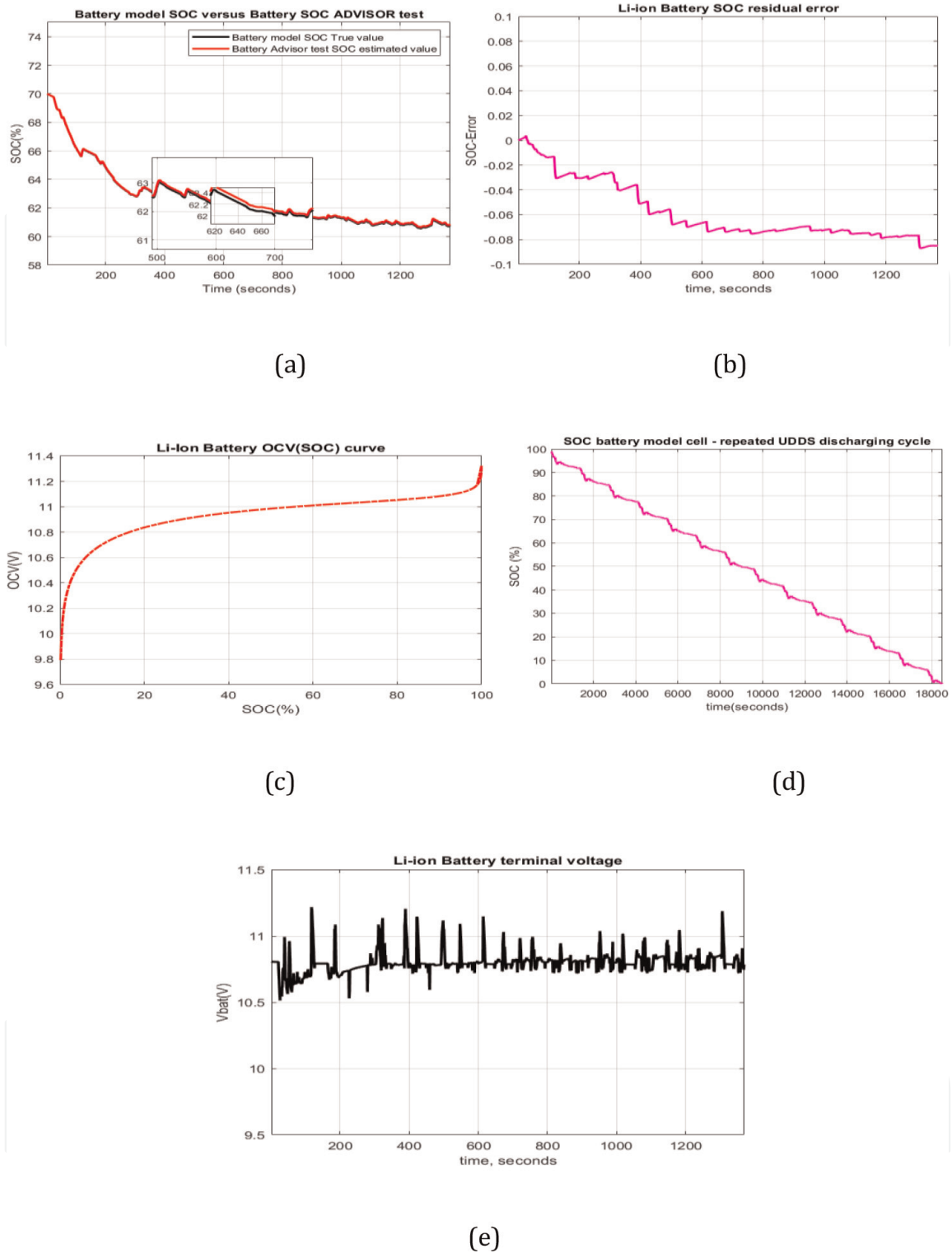


**Figure 9.** (a) Li-ion battery 3RC ECM model SOC versus battery ADVISOR simulator estimated; (b) SOC residual error; (c)  $OCV = f(SOC)$  curve for 5 hours full discharge of the battery to a UDDS driving multi-cycles; (d) SOC for a full battery discharge SOC; (e) SOC for a single UDDS driving cycle discharging input profile (1370 seconds).

insight on OCV(SOC) impact on battery SOC accuracy. Finally, a combined ARX Rint-3RC ECM – ANFIS OCV(SOC) model structure is investigated. The Simulink diagram with all these alternative modeling techniques is shown in **Figure 8**. To build a single-input single-output (SISO) ARX model, the system identification MATLAB toolbox and Simulink are the most precious tools [13]. Also, for good documentation,

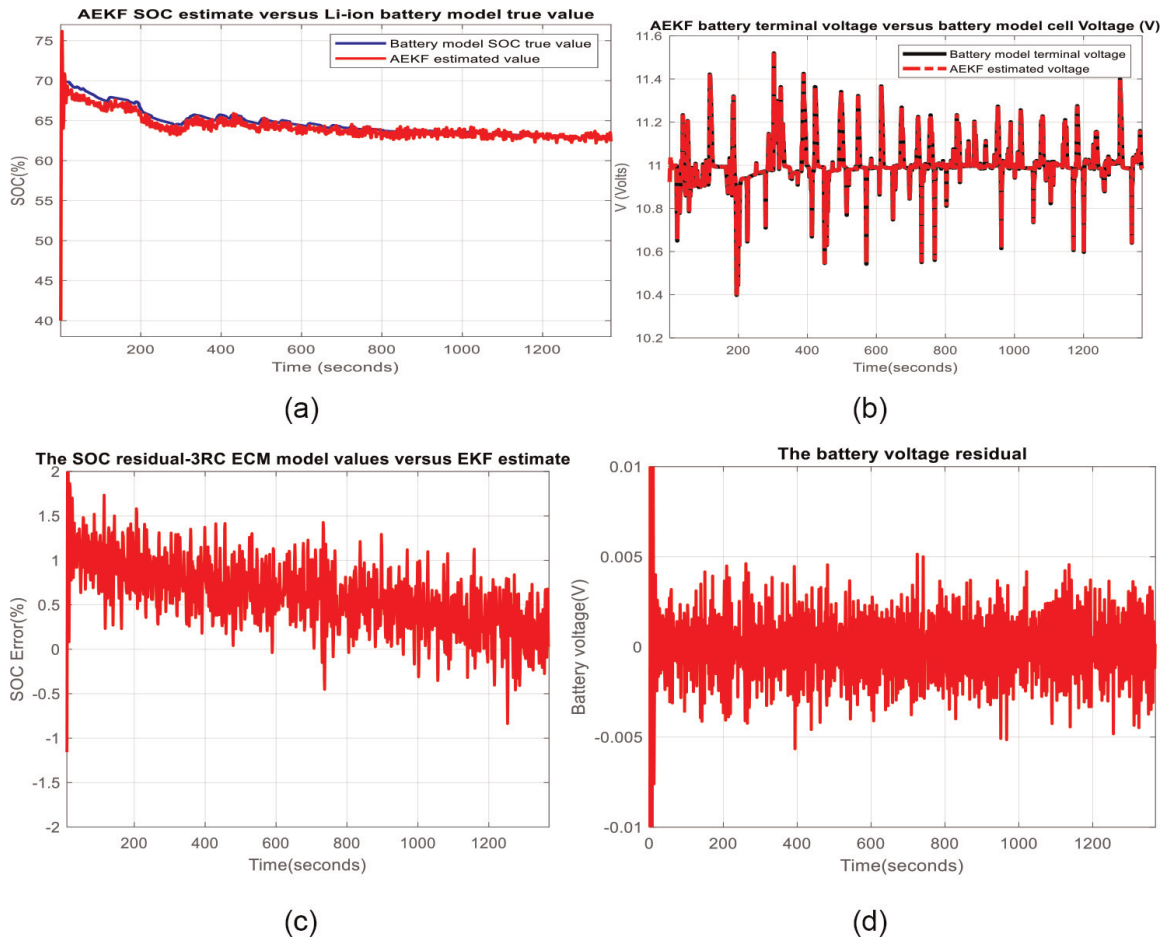


**Figure 10.**

(a) SOC voltage; (b) battery terminal voltage versus AEKF estimated. (c) Terminal voltage residual error; (d) SOC residual error.

a piece of valuable information about ARX models is provided in the references [10–13, 31]. MATLAB’s arx command is helpful to generate and estimate the models’ parameters from the input-output data sets. This MATLAB command is a routine based on a prediction-error least-squares method and specified polynomial orders to estimate the parameters of ARX polynomial discrete-time models. The model properties include covariances (parameter uncertainties) and goodness of fit between the estimated and measured data. Fundamental work on systems identification is done in [31]. The MATLAB implementation and simulations of SISO polynomial ARX models can be performed on any recent MATLAB platforms available online at [www.mathworks.com/help/ident/ref/arx.html](http://www.mathworks.com/help/ident/ref/arx.html) [13]. A “trial and error” procedure is considered to select the most suitable ARX model order. This procedure is repetitive until the best match of the data set is found, provided by the following status indicators:

- Fit to data estimation (prediction focus)
- Final prediction error (FPE)
- Mean square error (MSE),

as recorded output data of ARX model. The ARX model can be represented in the discrete state-space by the following polynomial with constant coefficients:



$$A(q)y_d(t) = B(q)u(t) + e(t) \quad (7)$$

where  $y_d(t)$  is the output dynamics part of the series circuit Rint-3RC, given by

$$y_d(t) = R_{int}u(t) + V_1(t) + V_2(t) + V_3(t) = v_d(t) \quad (8)$$

where the voltages  $V_1(t)$ ,  $V_2(t)$ , and  $V_3(t)$  are given in Eq. (1), Eq. (2), and respectively Eq. (3). The Rint-3RC circuit input  $u(t)$  denotes the battery charging and discharging current input (e.g., UDDS driving cycle input current profile). The linear discrete time polynomials  $A(q)$  and  $B(q)$  in Eq. (7) have the degrees  $n_a$  (poles), respectively  $n_b$  (zeroes) and are described as,

$$A(q^{-1}) = 1 + a_1q^{-1} + \dots + a_{n_a}q^{-n_a} \quad (9)$$

$$B(q^{-1}) = b_1q^{-1-n_k} + \dots + b_{n_b}q^{-n_b-n_k+1} = q^{-n_k}(b_1q^{-1} + \dots + b_{n_b}q^{-n_b+1}) \quad (10)$$

where  $n_k$  designates an integer number of samples as a track record of pure transport signal flow delay between the system input-output measurement sensors. Also,  $u(t)$  and  $y_d(t)$  in Eq. (7) denote the Rint-3RC ECM input, respectively, its output at the discrete instant  $t = kT_s, k \in \mathbb{Z}^+$ ,  $q$  is a forward shift operator, i.e.,  $q(u(t)) = u(t+1)$ ,  $q(y_d(t)) = y_d(t+1)$ , and  $q^{-1}$  is backward shift operator, i.e.,  $q^{-1}(u(t)) = u(t-1)$ ,  $q^{-1}(y_d(t)) = y_d(t-1)$ .  $T_s$  represents the sampling period, and  $e(t)$  term denotes the white noise disturbance value at the discrete instant  $t$ . The values of  $n_a$  and  $n_b$  that signify the degrees of the polynomials  $A(q)$  and  $B(q)$ , respectively, are set to the arguments in the syntax of the specific MATLAB arx command from Control Systems Identification MATLAB Toolbox. To use MATLAB Simulink to build the 3RC ECM battery model based on ARX model of the Rint-3RC electrical circuit dynamic part, a transfer function representation of the linear discrete-time polynomial ARX model is required. Some of MATLAB simulations results obtained after the use for ARX Rint-3RC ECM model implementation of the identification systems toolbox arx command are shown below. Discrete-time ARX (2,2,1) (i.e., ARX ( $n_a = 2, n_b = 2, n_k = 1$ )) model [10, 12, 13]:

$$A(z)y_d(t) = B(z)u(t) + e(t) \quad (11)$$

$$A(z) = 1 - 1.121z^{-1} + 0.2837z^{-2}, a_1 = -1.121, a_2 = 0.2837 \quad (12)$$

$$B(z) = 0.006972z^{-1} - 0.005292z^{-2}, b_1 = 0.006972, b_2 = -0.005292 \quad (13)$$

Sample time: 1 seconds, Parameterization: polynomial orders:  $n_a = 2, n_b = 2, n_k = 1$ , Number of free coefficients: 4, Status: Estimated using ARX on time-domain data, Fit to estimation data: 33.89% (simulation focus), FPE: 0.007562, MSE: 0.004557.

**Remark:** Since the roots of the characteristic equation  $A(z^{-1}) = 0$  are equal to  $0 < z_1 = 0.735 < 1, < 0$  and  $z_2 = 0.385 < 1$ , then the dynamic part of the 3RC ECM model is stable. The Simulink model of the ARX Rint-3RC ECM dynamic model part is integrated into the overall Simulink diagram shown in **Figure 8**, and the MATLAB simulation results for the new Li-ion battery SAFT accurate model implementation are presented in **Figure 11** for the ARX model of Rint-3RC ECM dynamic part voltage versus the voltage measurement values. In **Figure 7**, the result of simulations is related to battery terminal voltage based on the original 3RC ECM model versus battery

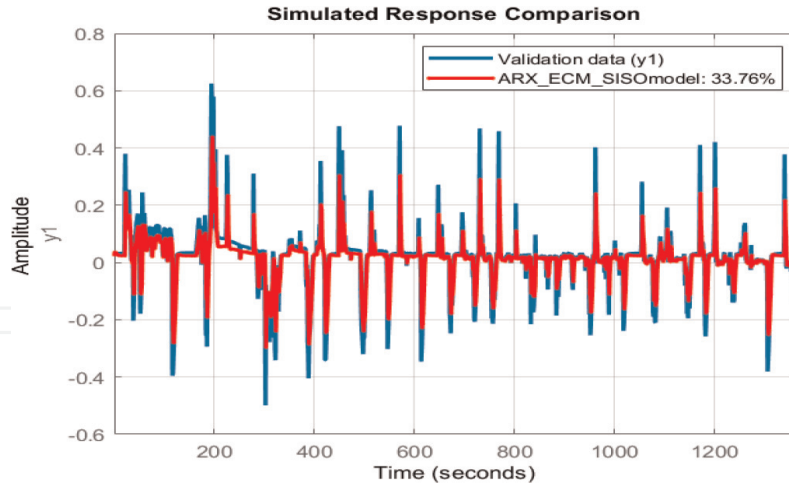


**Figure 11.**  
 The ARX – ECM model of 3RC ECM dynamic part voltage- MATLAB simulation result for validation.

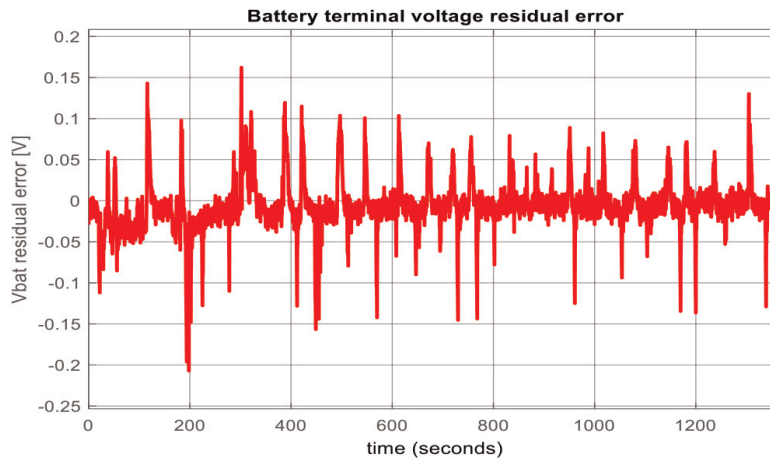


**Figure 12.**  
 Battery terminal voltage residual error.

terminal voltage in the integrated structure with ARX Rint-3RC ECM, the dynamic part model. For a good visualization of battery accuracy performance, the residual voltage between two previous voltages is depicted in **Figure 12**.

According to Eq. (4) and Eq. (6), an overall discrete-state space representation for the integrated ARX model structure of 3RC ECM SAFT Li-ion battery model can be written as follows:

$$soc(k + 1) = soc(k) - \frac{\eta T_s u(k)}{C_{nom}}, soc(0) = SOC_{ini} \quad (14)$$

$$y(k) = -V_d(k) + V_{OCV}(k) = -ARX(u(k)) + OCV(soc(k)) \quad (15)$$

where  $y_d(k) = V_d(k)$  represents the output voltage of the dynamic part Rint-3RC ECM, and  $u(k) = i(k)$  the input current profile of the battery. Also, a detailed discrete-time state-space representation has the following form:

$$x(k + 1) = Ax(k) + Bu(k) + w(k) \quad (16)$$

$$y(k) = Cx(k) + v(k) \quad (17)$$

where

$$A = \begin{bmatrix} 1 & 0 & 0 \\ 0 & a_1 & a_2 \\ 0 & 0.5 & 0 \end{bmatrix}, \quad B = \begin{bmatrix} -\frac{\eta T_s}{C_{nom}} \\ b_1 \\ 0 \end{bmatrix}, \quad C = \begin{bmatrix} \frac{OCV(soc(k))}{soc(k)} & c_1 & c_2 \end{bmatrix}, \quad (18)$$

$x(k) = \begin{bmatrix} soc(k) \\ x_1(k) \\ x_2(k) \end{bmatrix}$ ,  $u(k) = i(k)$  and represent the battery state vector and input

current driving cycle profile, respectively. The components  $x_1(k)$  and  $x_2(k)$  of the state vector describe the Rint-3RC ECM dynamics part of all three parallel polarization cells, and  $y(k)$  is the predicted battery terminal voltage. The new model parameters have the following values:  $a_1 = 1.121$ ,  $a_2 = -0.5674$ ,  $c_1 = 0.058578$ , and  $c_2 = -0.08467$ . The advantage of the new discrete-time state-space representation compared with 3RC ECM battery original model is its third-order simplified structure. This structure is used to estimate the battery SOC using an AEKF SOC state estimator

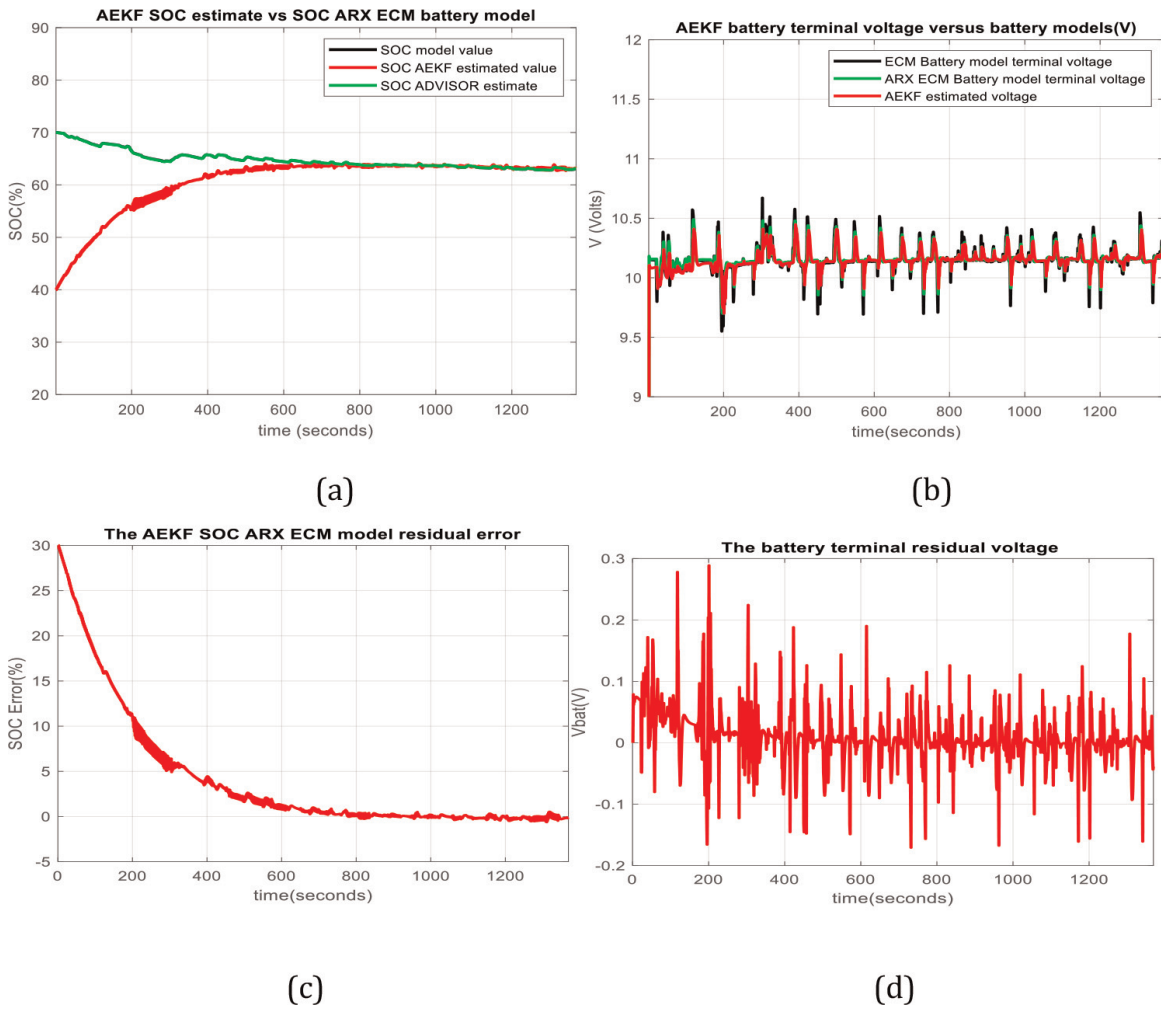


**Figure 13.** (a) The battery SOC true values versus SOC AEKF estimated values and SOC ADVISOR estimate for  $SOC_{ini} = 40\%$ ; (b) AEKF battery terminal voltage versus battery ARX ECM and 3RC ECM models terminal voltages; (c) SOC battery residual between ARX model SOC and AEKF SOC estimator; (d) terminal voltage error between ARX model and AEKF estimator.

and then to compare its accuracy performance with 3RC ECM Li-ion battery original model. For comparison purposes, the MATLAB simulation results of AEKF SOC estimator based on ARX battery model are shown in **Figure 13**. To also highlight the robustness of the AEKF SOC estimator to the changes in the initial value of battery SOC, in **Figure 13a** is depicted the battery SOC true values versus SOC AEKF estimated values and SOC ADVISOR estimate for an  $SOC_{ini} = 40\%$ . The simulation results reveal an excellent robustness and SOC accuracy of the adopted AEKF SOC estimator. Moreover, the simulation results are shown in **Figure 13b–d** that highlight the accuracy of battery terminal voltage of ARX ECM model compared with 3RC ECM and AEKF SOC estimator based on ARX model, as well as both residuals SOC and battery terminal voltage.

### 3. ANFIS Li-ion battery model design for dynamic part Rint-3RC ECM and OCV(SOC) nonlinear block

As an alternative to 3RC ECM and ARX battery models, the ANFIS modeling techniques are based on specific MATLAB commands provided by fuzzy logic toolbox and based on fuzzy inference tuning procedures [14–16]. The Sugeno-type inference system FIS is tuned based on an input-output training data set collected in open-loop from 3RC ECM Li-ion battery model. From our most recent preliminary results in the Li-ion battery field, modeling and SOC estimators disseminated in [12, 25, 26], an interesting state-of-the-art analysis of similar SOC AEKF estimators performance reported in the literature is done in terms of statistical performance criteria values, such as root mean square error (RMSE), mean square error (MSE), mean absolute error (MAE), standard deviation (std), mean fundamental percentage error (MAPE), and R2 (R-squared). Among three SOC Li-ion battery estimators, the AEKF, adaptive unscented Kalman filter (AUKF), and particle filter (PF) SOC estimators, the AEKF proved that is the most suitable for HEVs applications [29].

#### 3.1 Detailed ANFIS Li-ion battery model design steps

##### 3.1.1 ECM hybrid and combined Li-ion battery models structures: Training phase and battery terminal voltage accuracy

A specific MATLAB function *anfis(trainingData)* that has as argument the *TrainingData* generates a single-output Sugeno fuzzy inference system (FIS) and tunes the system parameters using the specified input-output training data. The FIS object is automatically generated using the grid partitioning method. The training algorithm uses a combination of the least-squares and back propagation gradient descent methods to model the training data. Also, the same MATLAB function could have a second argument called *options* with the syntax *anfis(trainingData, options)* and tunes an FIS using the specified trainingData and options. Using this syntax, the user can select an initial FIS object to tune, validate the data to prevent overfitting to training data, the training algorithm options, and display training progress information. In the last two decades, an impressive amount of research was done by researchers, developers, and implementers in the artificial intelligence field to develop a robust theoretical background on neural network architectures, fuzzy logic design, and ANFIS modeling approach, as well as to create the most suitable

algorithms and techniques to be implemented in an extensive palette of applications [14, 18]. The following summarizes some of the key lines of MATLAB code that are much easier for MATLAB readers and users to understand a quick implementation of the online generation of the ANFIS model based exclusively on the input-output measurement data set suggested in [14]. The MATLAB implementation steps required to generate an ANFIS plant/process model, the actions that guide the reader/implementer are:

Step 1: Set up the driving cycle profile for Li-ion battery as input  $u$ , and the battery SOC ( $y_1$ ) and terminal voltage ( $y_2$ ) as battery outputs; The Li-ion battery input-output measurements data set will be collected from a 3RC ECM original battery model given by Eq. (1)–Eq. (7) from previous section through several extensive simulations conducted on MATLAB platform.

Step 2: Generate the ANFIS model grid partition method-based options using the specific MATLAB function:

```
options = genfisOptions('GridPartition')
options.NumMembershipFunctions = 5 or greater than this
```

Step 3: Construct the FIS input attached to the battery SOC and terminal voltage

```
in_fis1 = genfis (u, y1, options)
```

```
in_fis2 = genfis (u, y2, options)
```

Step 3: Select for training the ANFIS model options

```
options = anfisOptions.
```

```
options.InitialFIS1 = in_fis1
```

```
options.InitialFIS2 = in_fis2
```

```
options.EpochNumber = 20 or greater to get a reasonable accuracy
```

Step 4: Construct the FIS output attached to the battery SOC and terminal voltage

```
out_fis1 = anfis ([u y1], options)
```

```
out_fis2 = anfis ([u y2], options)
```

Step 5: Plot the input-output measurements data set versus input-output of both ANFIS models

```
plot (u, y1, u, evalfis (u, out_fis1))
```

```
plot (u, y2, u, evalfis (u, out_fis2))
```

```
legend ('trainingData', 'ANFIS Output').
```

The previous steps must be adapted to generate both ANFIS models of the Rint-3RC ECM dynamic part and the OCV(SOC) nonlinear function. The MATLAB simulation results are depicted in Figure. **Figure 14a** presents the ANFIS Rint-3RC ECM dynamic part model output and voltage training data set measurements, and **Figure 14b** shows only the ANFIS model output. The impact on battery terminal voltage accuracy using the ANFIS -ECM model compared with ARX -ECM developed in the last Section 2.1.4 is shown in **Figure 14c**. The accuracy of ANFIS -ECM model is revealed in **Figure 14d**, which presents the battery terminal voltage residual.

Also, for building some interesting Li-ion SAFT battery structures, an ANFIS model is developed for OCV(SOC) nonlinear function block in **Figure 15a** for training data phase, and in **Figure 15b** for OCV(SOC) ANFIS output model. Both ANFIS models are based on a repeated UDDS driving cycles input current profile for almost 5 hours to assure a large interval of input-output data set measurements for SOC, OCV, and battery dynamic part voltage. The impact of OCV(SOC) ANFIS block on battery terminal voltage accuracy based on 3RC ECM is revealed in **Figure 15c** and **d**. In **Figure 15c** it is very difficult to distinguish between ECM battery terminal voltage

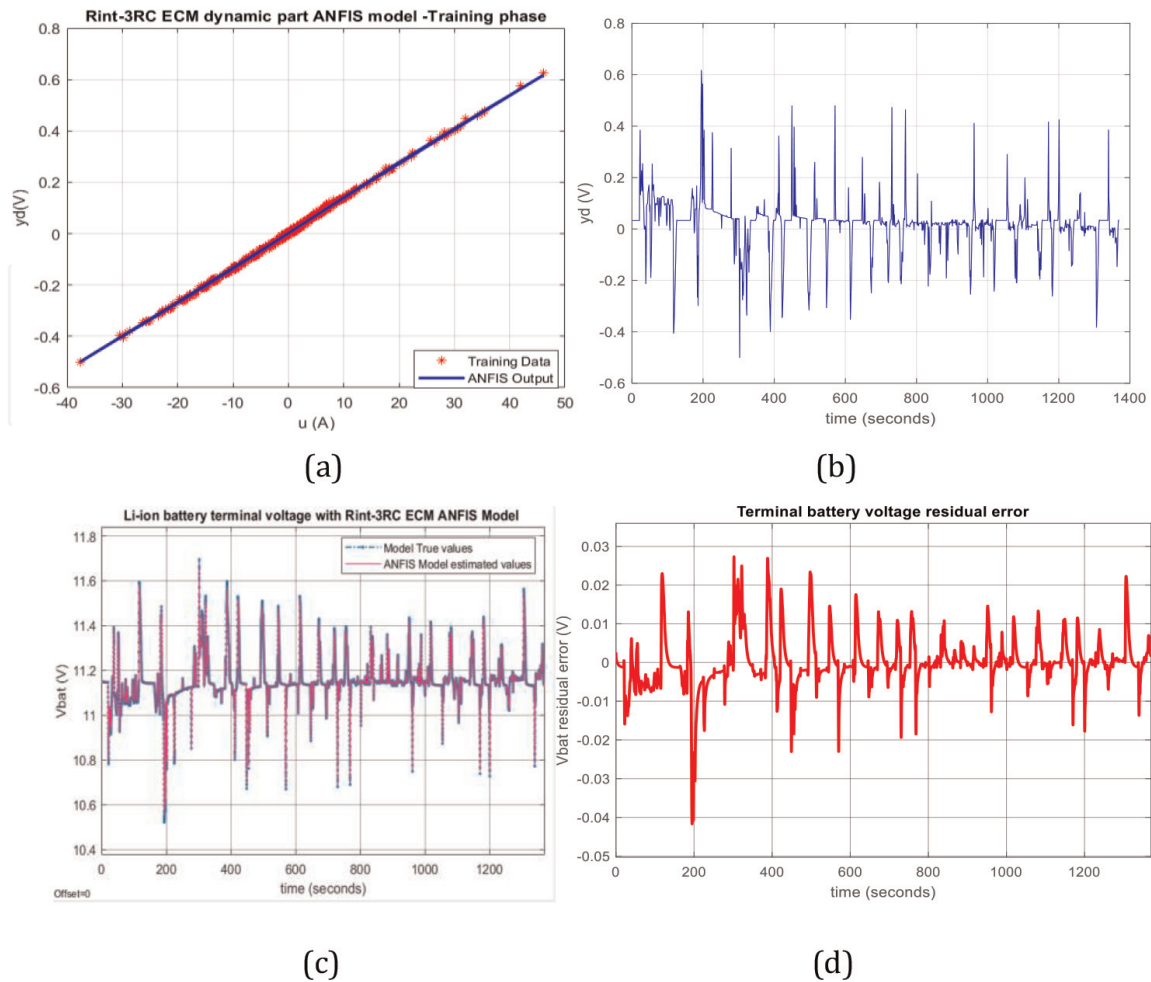


**Figure 14.** (a) ANFIS ECM dynamic part model output and voltage training data set measurements; (b) Rint-3RC ECM dynamic part ANFIS model  $y_d$  circuit output; (c) terminal battery voltage  $V_{bat}$  with Rint-3RC ECM dynamic part ANFIS model (ANFIS-ECM); (d) terminal voltage residual error.

graph and the second one ECM Li-ion battery terminal voltage that integrates the OCV(SOC) block ANFIS model due to the high ANFIS OCV(SOC) model block accuracy. The reader can have a better insight on the battery terminal voltage accuracy in **Figure 15d** that reveals a very small battery terminal voltage residual error compared with the ARX ECM dynamic part battery model terminal voltage shown in previous **Figure 14d**.

Let us discuss why the ANFIS battery integrated model is the most suitable to build hybrid integrated battery Li-ion structures in terms of high accuracy.

An exciting hybrid battery Li-ion structure can incorporate into the ARX ECM dynamic part model and an ANFIS OCV(SOC) nonlinear block model. The MATLAB simulations result of the Li-ion battery hybrid structure is presented in **Figure 16a** and **b**.

A rigorous analysis of MATLAB simulation results from **Figure 15c** and **Figure 15d** shows a high battery terminal voltage accuracy compared with the battery hybrid structure, as can be seen in **Figure 16a** and **b**.

The last combined battery structure consists of two ANFIS models, the first one for Rint-3RC ECM active battery part and the second one that replaces the Li-ion SAFT ECM SUN OCV(SOC) nonlinear block with an ANFIS model block. The MATLAB simulation results are depicted in the **Figure 17a** and **b**.

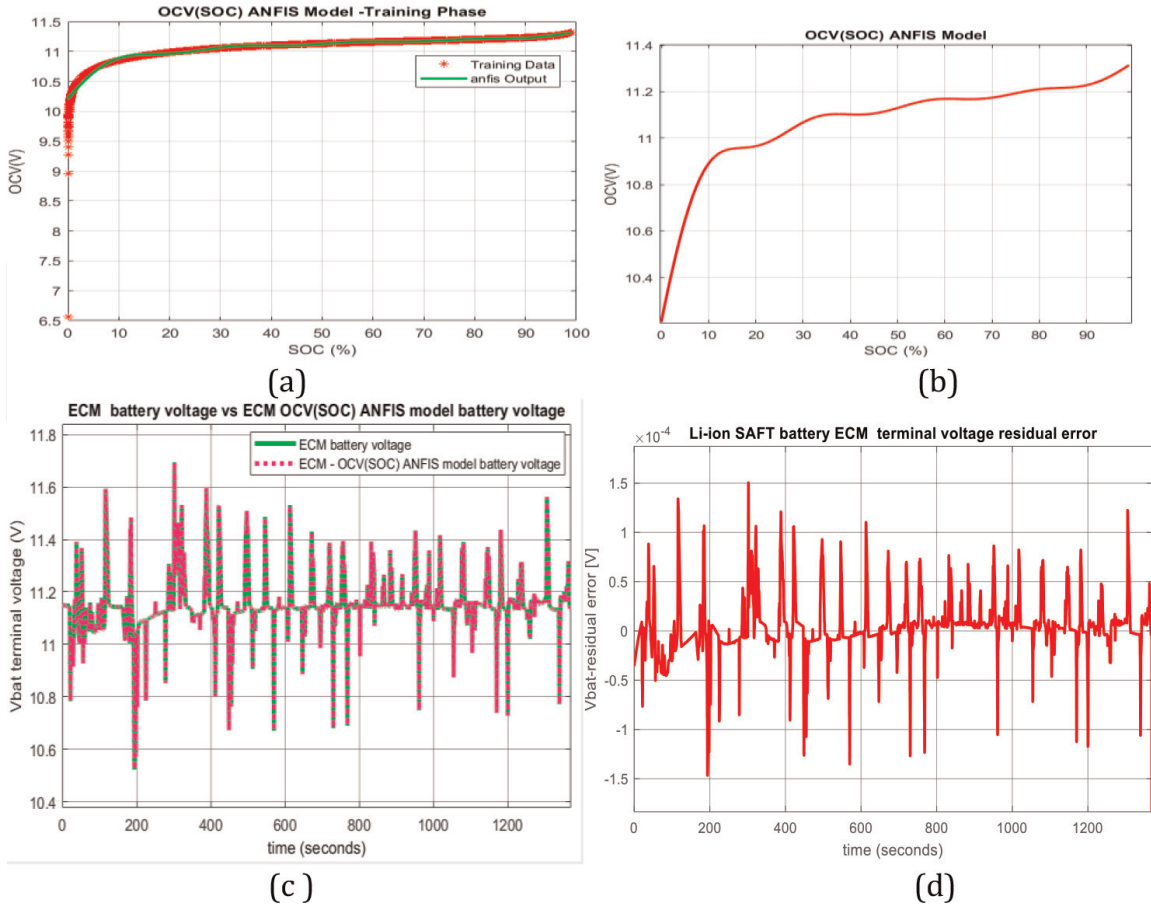


**Figure 15.** (a)  $OCV = f(SOC)$  ANFIS model versus OCV measurements; (b)  $OCV = f(SOC)$  ANFIS model; (d) ECM Li-ion SAFT battery terminal voltage versus ECM-OCV(SOC) ANFIS model ( $R_{int}$ -3RC -ANFIS) terminal battery voltage; (e) ECM Li-ion SAFT battery terminal voltage residual error versus ECM-OCV(SOC) ANFIS model ( $R_{int}$ -3RC – ANFIS) integrated structure.

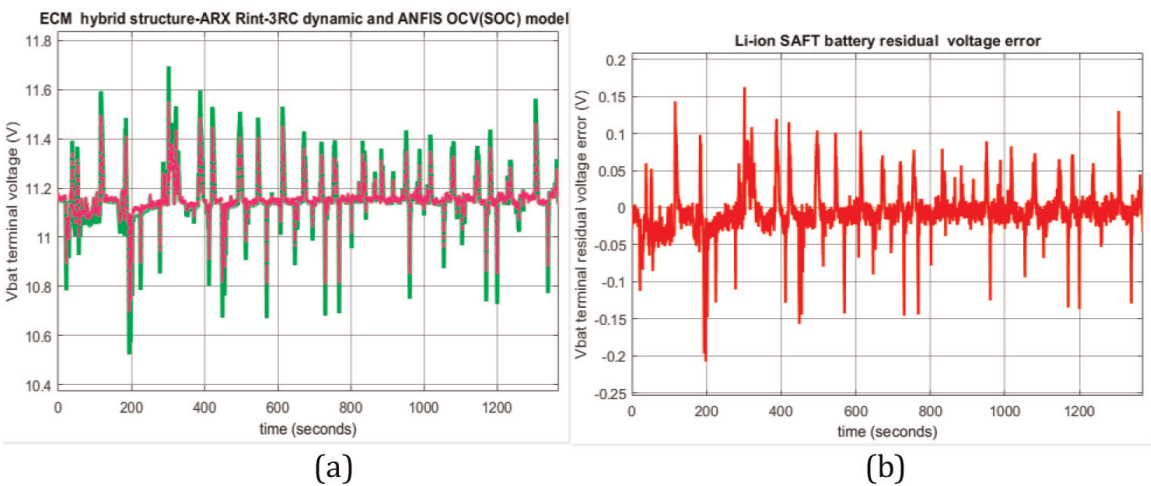


**Figure 16.** (a). ECM Li-ion SAFT hybrid structure – ARX  $R_{int}$ -3RC dynamic part and ANFIS OCV (SOC) nonlinear block model (ARX-ANFIS); (b) Li-ion SAFT battery terminal residual voltage error for hybrid structure.

The voltage accuracy performance revealed by simulation results from **Figure 17a** and **b** seems to be better than the previous hybrid ARX and ANFIS battery structure. Still, it is slightly inferior compared with the design that integrates only the ANFIS model for SOC(OCV) nonlinear battery block.

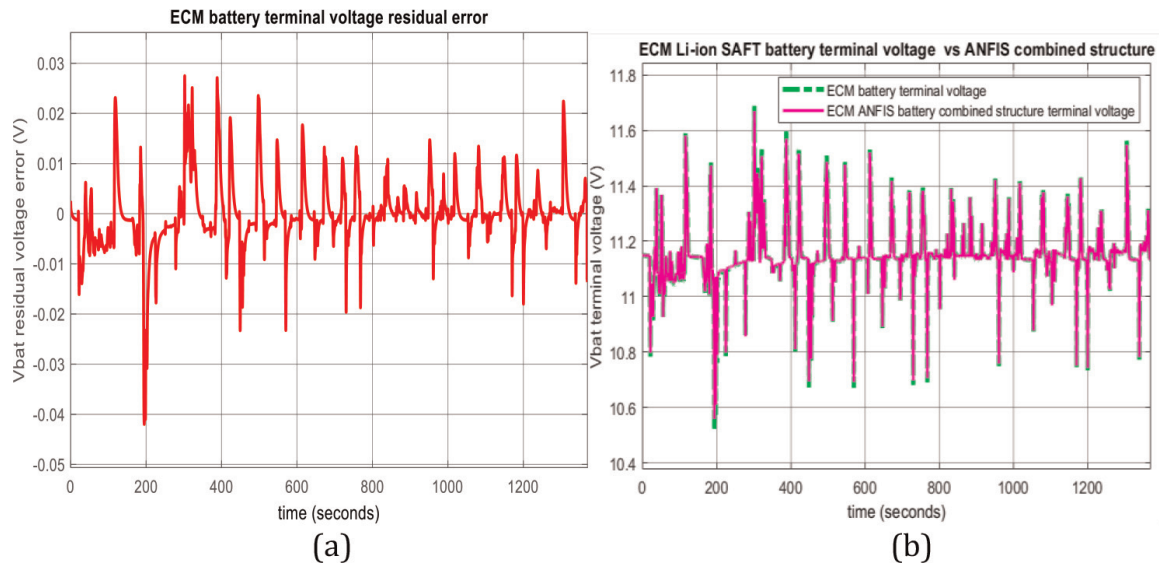


**Figure 17.**

(a) ECM Li-ion SAFT battery terminal voltage versus ECM ANFIS combined structure terminal voltage; (b) ECM Li-ion SAFT battery terminal residual voltage error for ECM ANFIS combined structure.

### 3.1.2 AEKF SOC estimator for ANFIS 3RC ECM SAFT Li-ion battery model: accuracy performance

For simplification purpose and SOC and battery terminal voltage accuracy, as alternative Li-ion 3RC ECM structure required to implement the AEKF SOC estimator on a MATLAB R2021b platform is considered the ANFIS 3RC ECM SAFT Li-ion battery model consisting of Rint-3RC ECM dynamic part block, and second ANFIS model attached to OCV(SOC) nonlinear block. The overall simplified ANFIS 3RC ECM battery model structure is described by the following equations:

$$soc(k + 1) = soc(k) - \frac{\eta T_s u(k)}{C_{nom}}, soc(0) = SOC_{ini} \quad (19)$$

$$y(k) = V_{OCV}(k) - V_d(k) = \left( \frac{anfis(soc(k))}{soc(k)} \right) soc(k) - anfis(u(k)) \quad (20)$$

In all the MATLAB simulations for implementing the AEKF SOC estimator are considered the following parameters values:

- SOC initial value = 0.4,

Covariance of estimated value of SOC,  $Phat = 1e-10$ ,

- Covariance process noise  $Qw = 0.01$ ,
- Measurement noise  $Rv = 0.001$ .
- $\alpha = 0.791$ ,  $r = 5$ .

The MATLAB simulations results are presented in **Figure 18a–c**. Similar to ARX model developed in previous chapter 2, in **Figure 18** the robustness of AEKF



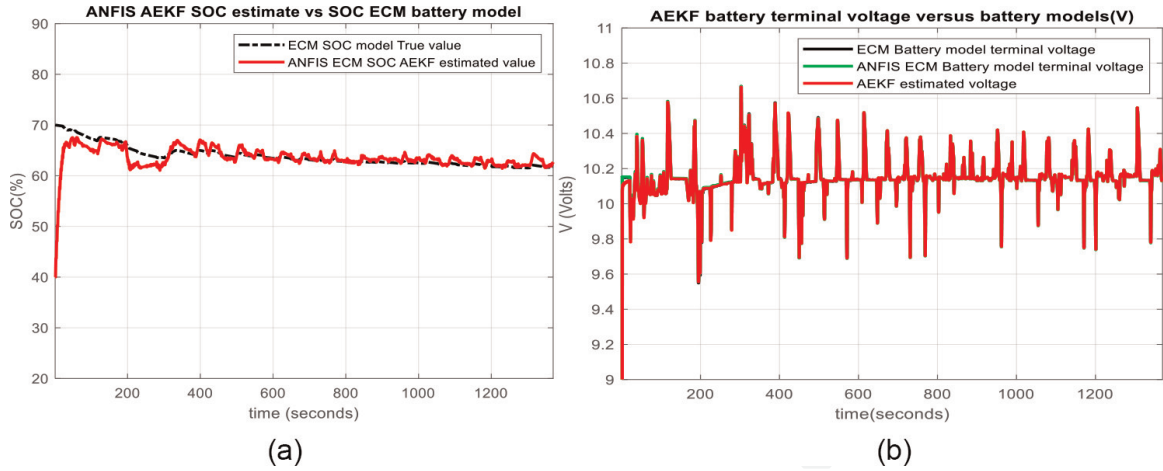


**Figure 18.** (a) Robustness of ANFIS AEKF SOC estimator to changes in SOC initial values from  $SOC_{ini} = 0.7$  to  $SOC_{ini} = 0.4$ ; (b) the ANFIS 3RC ECM Li-ion battery OCV voltage accuracy.

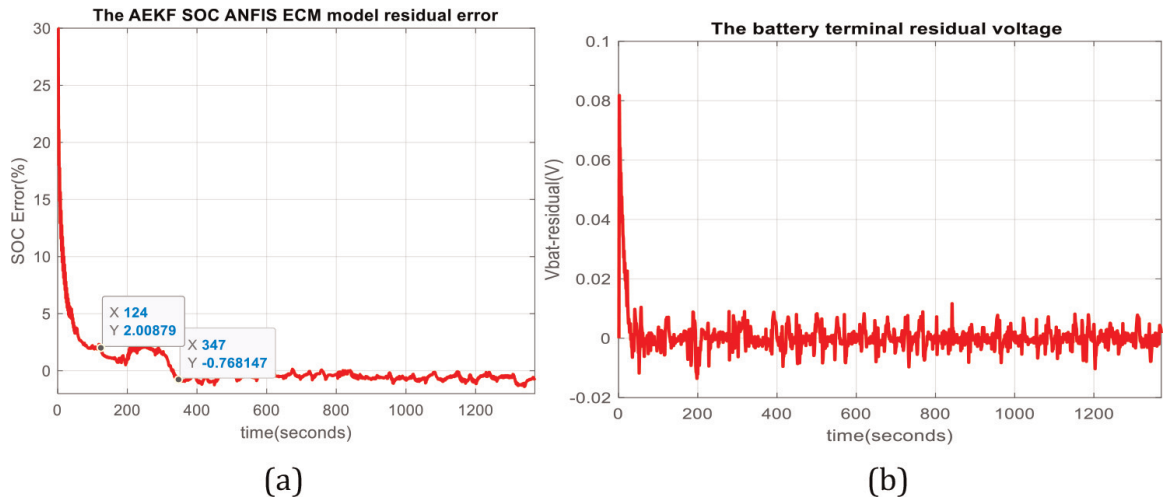


**Figure 19.** (a) The ANFIS 3RC ECM Li-ion battery SOC residual error; (b) the ANFIS 3RC ECM Li-ion battery terminal voltage residual error with respect with the battery terminal voltage estimated by AEKF.

SOC estimator to changes in the battery SOC initial values from  $SOC_{ini} = 0.7$  to  $SOC_{ini} = 0.4$  is shown. In **Figure 18b** the predicted values of battery terminal and OCV voltages cell by AEKF and ANFIS are compared with 3RC ECM true values.

The battery SOC and terminal voltage accuracy are revealed in **Figure 19a** and **b**, respectively, based on SOC and battery terminal voltage residuals.

### 3.2 Discussion: ANFIS models and AEKF SOC estimator performance analysis

Based on the information accessible from the battery SOC and terminal voltage residual errors presented in the first two subsections of Section 3, more precisely the MATLAB simulation results and the statistics criteria values RMSE, RSE, MAE, MAPE, collected in **Table 2**, can be made a rigorous performance analysis of both ANFIS models and AEKF SOC estimator.

### 3.2.1 ANFIS models performance accuracy analysis

The performance analysis is made on the information provided by the battery terminal voltage residuals errors. The MATLAB simulation results reveal a battery terminal voltage prediction accuracy for ANFIS Rint-3RC ECM dynamic part model of an absolute residual error less than 0.03 volts and greater than  $-0.04$  volts, compared with ARX model of same structure that is situated in the range  $(-0.2, 0.15)$  volts. The voltage error of OCV(SOC) ANFIS model is very small ranged inside the interval  $(-1.5 \times 10^{-4}, 1.5 \times 10^{-4})$  volts. For the ANFIS combined structure (ANFIS-ANFIS), the residual error remains in the same range as Rint-3RC ECM dynamic part model, i.e.,  $(-0.04, 0.03)$  volts.

### 3.2.2 AEKF based on ANFIS combined model (ANFIS-ANFIS) performance accuracy analysis

The performance analysis is made on the information provided by the battery SOC and terminal voltage residuals errors shown in **Figure 19a** and **b**. During the steady state, more precisely after 347 seconds, the SOC residual error is less than 1% smaller

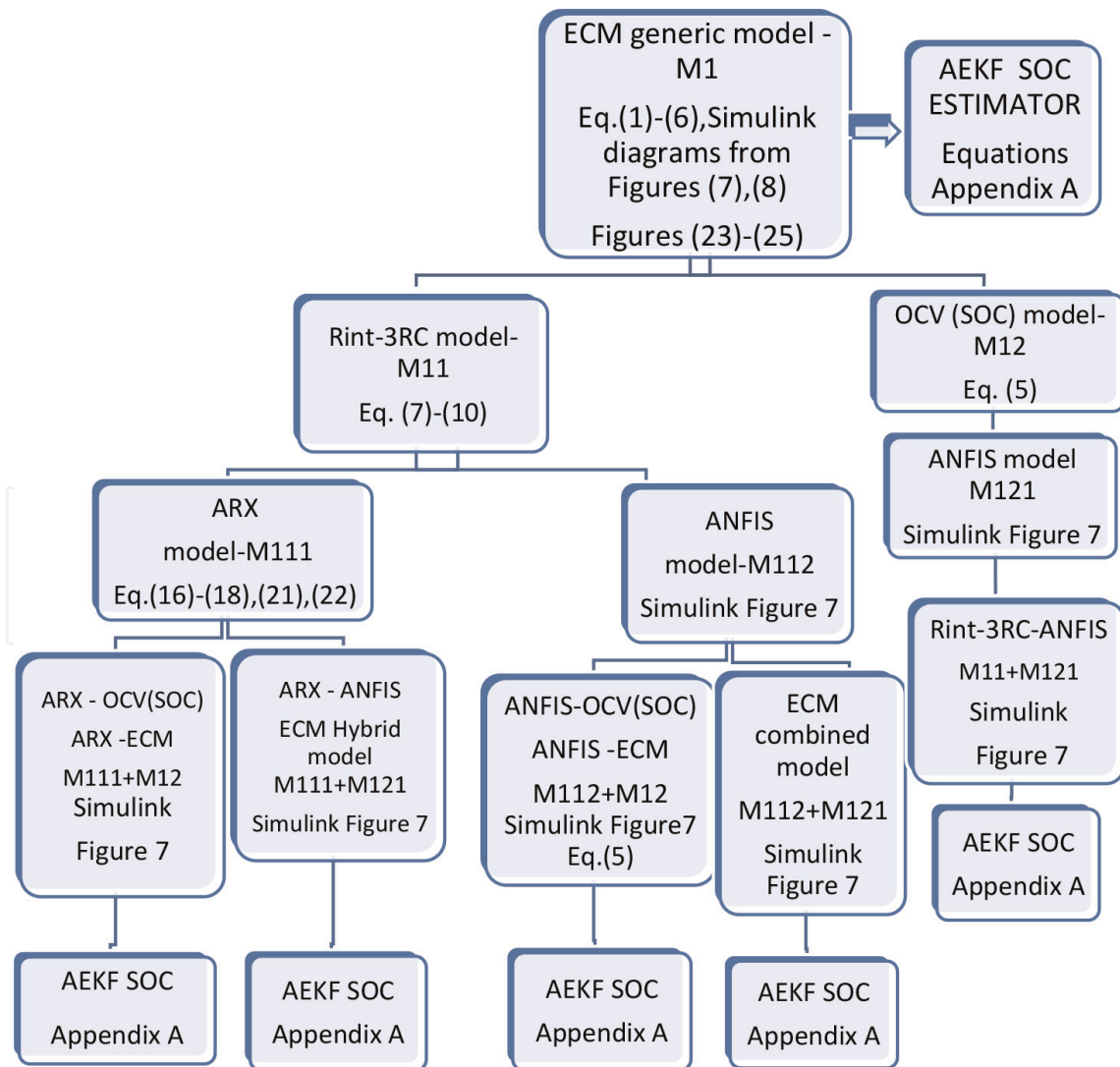


**Figure 20.**  
 System-level flowchart diagram.

than usual SOC residual error of 2% value reported in the literature field. Since the SOC residual error of AEKF based on ARX ECM battery model that is less than 1% during the steady state after 600 s, as is shown in **Figure 13c**, it is obviously that the AEKF based on ANFIS battery model performs better. For a complete information about the suitability of AEKF SOC estimator based on ANFIS battery model is built in the **Table 2**, which incorporates all the statistics of criteria values RMSE (IC1), MSE (IC2), MAE (IC3), and MAPE (IC4), the most common criteria that have been used in the literature field to measure model performance and select the best model from a set of potential candidate models [7, 29, 30]. Comparing both statistics criteria values (third and fourth columns) is straightforward that the AEKF SOC estimator based on ANFIS battery model performs better than AEKF SOC estimator based on ARX battery model.

By comparing the terminal battery voltage residuals shown in **Figure 12** for AEKF based on ARX model and AEKF based on ANFIS model depicted in **Figure 19b**, they are ranged inside the intervals  $(-0.2, 0.3)$  volts and  $(-0.01, 0.08)$  volts, respectively; thus, the second SOC estimator based ANFIS battery model performs better than the first one. Based on the performance analysis of SOC accuracy, robustness to changes in SOCini value and terminal battery voltage prediction accuracy it can conclude that the AEKF SOC estimator based on ANFIS model is the most suitable SOC estimator for HEVs/EVs applications.

A system-level flowchart/flow diagram is shown in **Figure 20**. It indicates the major steps involved in the key sections of the last two chapters to provide an overview of the differences in steps between generic ECM, ARX ECM, ANFIS ECM, hybrid (ARX-ANFIS), and combined (ANFIS-ANFIS) models.

A detailed description for each small block of the overall diagram of the models along with a flow of the equations is also considered in the overall diagram shown in **Figure 20**.

## 4. Conclusions

This research paper has opened a new Li-ion battery modeling research direction in the HEV BMS applications field by performing several investigations on ARX and ANFIS alternative accurate battery models with a high impact on improving the battery SOC estimators' accuracy and their robustness, design, and real-time implementation in MATLAB and Simulink environments.

The effectiveness of the modeling and SOC estimation strategies is demonstrated through an extensive number of simulations in a MATLAB R2021b software environment. The preliminary simulation results are encouraging, and extensive investigations will be done in future work to extend the applications area. The performance analysis from the last section reveals that ANFIS battery models overpass the second-order linear ARX polynomial battery model in terms of SOC and terminal voltage accuracy and by their capability and suitability to simplify the battery model structure and build robust and accurate SOC Li-ion battery estimators with a high terminal voltage prediction accuracy. The AEKF SOC estimator accuracy based on combined ANFIS model structure is also very accurate compared with AEKF SOC estimator based on ARX dynamic part model with the SOC absolute value lower than 1%, better than the usual 2% SOC value reported in the literature field. Both alternative models are based only on the measurement input-output data set collected by a data acquisition (DAQ) system incorporated in the BMS of HEVs. Besides, the battery SOC and output voltage signals' accuracy is not affected by noise as long as the AEKF SOC estimator is very robust.

## Conflict of interest

The authors declare no conflict of interest.

## Abbreviations/Acronyms

EV	electric vehicle
HEV	hybrid electric vehicle
BMS	battery management system
FTP-75	Federal test procedure at 75 F
UDDS	Urban Dynamometer Driving Schedule
OCV	open-circuit voltage
SUN-OCV	Shepherd, Unnewehr universal and Nernst open-circuit voltage
SOC	state of charge
ARX	autoregressive exogenous
NREL's	ADVISOR National Renewable Energy Laboratory Advanced Vehicle Simulator
AEKF	adaptive extended Kalman filter
ANFIS	adaptive neuro-fuzzy inference system
ECM	equivalent circuit model
MPC	model predictive control
3RC	ECM third-order RC ECM
Rint-3RC	ECM third-order internal resistance RC ECM
FDI	fault detection isolation
RMSE	root mean square error
MSE	mean square error
MAE	mean absolute error
MAPE	mean absolute percentage error
std.	standard deviation
$R^2$	R-squared
ARX-ECM	Rint-3RC replaced by ARX model
Rint-3RC-ANFIS	OCV(SOC) block replaced by ANSIM model
ARX-ANFIS	Rint-3RC replaced by ARX and OCV (SOC) by ANFIS (hybrid structure)
ANFIS-ANFIS	Rint-3RC replaced by ANFIS and OCV (SOC) by ANFIS (combined structure)

IntechOpen

### **Author details**

Roxana-Elena Tudoroiu<sup>1</sup>, Mohammed Zaheeruddin<sup>2</sup>, Nicolae Tudoroiu<sup>3\*</sup>  
and Sorin Mihai Radu<sup>1</sup>

1 University of Petrosani, Petrosani, Romania


2 Concordia University from Montreal, Montreal, Canada

3 John Abbott College, Sainte-Anne-de-Bellevue, Canada

\*Address all correspondence to: ntudoroiu@gmail.com

### **IntechOpen**

---

© 2022 The Author(s). Licensee IntechOpen. This chapter is distributed under the terms of the Creative Commons Attribution License (<http://creativecommons.org/licenses/by/3.0>), which permits unrestricted use, distribution, and reproduction in any medium, provided the original work is properly cited. 

## References

- [1] Xia B, Zheng W, Zhang R, Lao Z, Sun Z. Mint: A novel observer for Lithium-ion battery state of charge estimation in electric vehicles based on a second-order equivalent circuit model. *Energies*. 2017;**10**(8):1150. DOI: 10.3390/en10081150 Available from: <http://www.mdpi.com/1996-1073/10/8/1150/htm>
- [2] Young K, Wang C, Wang LY, Strunz K. Electric vehicle battery technologies—chapter 2. In: Garcia-Valle R, JAP L, editors. *Electric Vehicle Integration into Modern Power Networks*. 1st, 9, and 325 ed. New-York, USA: Springer Link: Springer-Verlag; 2013. pp. 15-26. DOI: 10.1007/978-1-4614-0134-6.ch.2
- [3] Farag M. Lithium-ion batteries. In: *Modeling and State of Charge Estimation*, (Thesis). Ontario, Canada: McMaster University of Hamilton; 2013. p. 169
- [4] Tudoroiu R-E, Zaheeruddin M, Radu SM. In: Louis Romeral Martinez TN, Prieto MD, editors. *New Trends in Electrical Vehicle Powertrains*, Vol. 4. London, UK: IntechOpen Limited; 2019. pp. 55-81. DOI: 10.5772/intechopen.76230.ch4
- [5] Plett GL. Extended Kalman filtering for battery management systems of LiPB-based HEV battery packs: Part 2. Modeling and identification. *Journal of Power Sources*. 2004;**134**:262-276. DOI: 10.1016/j.jpowsour.2004.02.032
- [6] Zhang R, Xia B, Li B, Cao L, Lai Y, Zheng W, et al. State of the art of Li-ion battery SOC estimation for electrical vehicles. *Energies*. 2018;**11**:1820
- [7] Tudoroiu R-E, Zaheeruddin M, Tudoroiu N, Radu S-M. SOC estimation of a rechargeable Li-ion battery used in fuel-cell hybrid electric vehicles—Comparative study of accuracy and robustness performance based on statistical criteria. Part I: Equivalent models. *Batteries*. 2020;**6**(3):42. DOI: 10.3390/batteries6030042
- [8] Wu C, Zhu C, Ge Y, Zhao Y. A review on fault mechanism and diagnosis approach for Li-ion batteries. *Journal of Nanomaterials*. 2015;**2015**:1-9. DOI: 10.1155/2015/631263
- [9] Tudoroiu N, Zaheeruddin M, Tudoroiu R-E, Radu S-M. Fault detection, diagnosis, and isolation strategy in Li-ion battery management systems of HEVs using 1-D wavelet signals analysis. In: Mohammady S, editor. *Wavelet Theory*. London, UK: IntechOpen; 2021. DOI: 10.5772/intechopen.94554. Available from: <https://www.intechopen.com/chapters/74031>
- [10] Yuan S, Wu H, Yin C. State of charge estimation using the extended Kalman filter for battery management systems based on the ARX battery model. *MDPI, Energies Journal*. 2013;**6**:444-470. DOI: 10.3390/en6010444
- [11] Uddina F, Tufaa LD, Yousifa SMT, Mauluda AS. Comparison of ARX and ARMAX decorrelation models for detecting model-plant mismatch. In: 4th International Conference on Process Engineering and Advanced Materials, *Procedia Engineering*. Vol. 148. Amsterdam, Nederland: Elsevier Ltd, ScienceDirect; 2016. pp. 985-991. DOI: 10.1016/j.proeng.2016.06.536
- [12] Tudoroiu N, Zaheeruddin M, Tudoroiu R-E. Modelling, identification, implementation, and MATLAB simulations of multi-input multi-output proportional integral-plus control strategies for a centrifugal chiller system.

- Int. J. Modelling, Identification and Control. 2020;**35**(1):64-91. DOI: 10.1504/ijmic.2020.10035847
- [13] MathWorks MATLAB Version R2019b On-Line Documentation, Available from: <https://www.mathworks.com/help/ident/ref/arx.html>
- [14] MathWorks MATLAB Version R2021b on-line Documentation, Neuro-Adaptive Learning and ANFIS. Available from: <https://www.mathworks.com/help/fuzzy/neuro-adaptive-learning-and-anfis.html>
- [15] Konsoulas Ilias S. Adaptive Neuro-Fuzzy Inference Systems (ANFIS) Library for Simulink. Available from: <https://www.mathworks.com/matlabcentral/fileexchange/36098-adaptive-neuro-fuzzy-inference-systems-anfis-library-for-simulink>, MATLAB Central File Exchange. [Accessed: January 19, 2022].
- [16] MathWorks MATLAB Version R2021b on-line Documentation, Neuro-Fuzzy Designer. Available from: <https://www.mathworks.com/help/fuzzy/neurofuzzydesigner-app.html>.
- [17] Bellali B, Hazzab A, Bousserhane IK, Lefebvre D. A decoupled parameters estimators for in nonlinear systems fault diagnosis by ANFIS. *International Journal of Electrical and Computer Engineering (IJECE)*. 2012;**2**(2):166-174. DOI: 10.11591/ijece.v2i2.221
- [18] Tudoroiu R-E, Zaheeruddin M, Tudoroiu N, Burdescu DD. MATLAB implementation of an adaptive neuro-fuzzy Modeling approach applied on nonlinear dynamic systems – A case study. In: *Proceedings of the Federated Conference on Computer Science and Information Systems*. Vol. 15. Poznan: ACSIS; 2018. pp. 577-583. DOI: 10.15439/2018F38
- [19] Nourani V, Uzelaltinbulat S, Sadikoglu F, Behfar N. Artificial intelligence based ensemble Modeling for Multi-Station prediction of precipitation. *Atmosphere*. 2019;**10**:80. DOI: 10.3390/atmos10020080
- [20] Chang F-J, Chang Y-T. Adaptive neuro-fuzzy inference system for prediction of water level in reservoir. In: *Advances in Water Resources*. Vol. 29. Amsterdam, Nederland: Elsevier Ltd; 2005. pp. 1-10. DOI: 10.1016/j.advwatres.2005.04.015
- [21] Mosavi A, Ozturk P, Chau K-W. Flood prediction using machine learning models: Literature review. *Water*. 2018;**10**:1536. DOI: 10.3390/w10111536
- [22] Huang C-L, Hsu N-S, Wei C-C, Lo C-W. Using artificial intelligence to retrieve the optimal parameters and structures of adaptive network-based fuzzy inference system for typhoon precipitation forecast Modeling. *Advances in Meteorology*. 2015;**9**:1-22. DOI: 10.1155/2015/472523
- [23] Chen S-H, Lin Y-H, Chang L-C, Chang F-J. The strategy of building a flood forecast model by neuro-fuzzy network. *Hydrological Processes*. 2006;**20**:1525-1540. DOI: 10.1002/hyp.5942
- [24] Ilias Konsoulas. Recurrent Fuzzy Neural Network (RFNN) Library for Simulink. Available from: <https://www.mathworks.com/matlabcentral/fileexchange/43021-recurrent-fuzzy-neural-network-rfnn-library-for-simulink>, MATLAB Central File Exchange. [Accessed: January 19, 2022]
- [25] Appiah R, Panford JK, Riverson K. Implementation of adaptive neuro fuzzy inference system for malaria diagnosis. Case study: Kwesimintsim polyclinic. *International Journal of Computer*

Applications India. 2015;**115**(7):33-37.  
DOI: 10.5120/20166-2284

[26] Jang J-SR. ANFIS: Adaptive-network-based fuzzy inference system. IEEE Transactions on System, Man, and Cybernetics. 1993;**23**:665-685. DOI: 10.1109/21.256541

[27] Karathanasopoulos A, Zaremba A, Osman M, Mikutowski M. Oil forecasting using artificial intelligence. Theoretical Economics Letters. 2019; **09**(07):2283-2290. DOI: 10.4236/tel.2019.97144

[28] Nahr ST, Pahlavani P, Amirkalayi A. A comparative study of adaptive neuro-fuzzy inference Systems in Object Detection of complex City scenes using digital aerial images and LiDAR data. Journal of the Indian Society of Remote Sensing. 2015;**43**(4):1-13. DOI: 10.1007/s12524-015-0457-1

[29] Tudoroiu R-E, Zaheeruddin M, Tudoroiu N, Radu S-M. SOC estimation of a rechargeable Li-ion battery used in fuel-cell hybrid electric vehicles—Comparative study of accuracy and robustness performance based on statistical criteria. Part II: SOC estimators. Batteries. 2020;**6**(3):42. DOI: 10.3390/batteries6030041

[30] Pham H. A new criterion for model selection. Mathematics. 2019;**7**(12):1215. DOI: 10.3390/math7121215

[31] Ljung L. System Identification: Theory for the User, Upper Saddle River. 2nd edition. NJ: Prentice-Hall PTR; 1999

[32] Zhang C, Jiang J, Zhang W, Sharkh SM. Estimation of state of charge of lithium-ion batteries used in HEV using robust extended Kalman filtering. Energies. 2012;**5**:1098-1115. DOI: 10.3390/en5041098

[33] Wu T, Wang M, Xiao Q, Wang X. The SOC estimation of power Li-ion battery based on ANFIS model. Smart Grid and Renewable Energy. 2012;**3**: 51-55. DOI: 10.4236/sgre.2012.31007